Structure-Function Relationships in Human Brain Development

by

Zeynep Mevhibe Saygin

B.Sc., Neuroscience
Brown University 2005

SUBMITTED TO THE
DEPARTMENT OF BRAIN AND COGNITIVE SCIENCES
IN PARTIAL FULFILLMENT OF THE REQUIREMENTS FOR THE DEGREE OF

DOCTOR OF PHILOSOPHY IN NEUROSCIENCE
AT THE
MASSACHUSETTS INSTITUTE OF TECHNOLOGY
September 2012

Author .....
Department of Brain and Cognitive Sciences
June 25, 2012

Certified by.....
John D. E. Gabrieli
Grover Hermann Professor in Health Sciences, Technology and Cognitive Neuroscience
Thesis Supervisor

Accepted by.....
Matthew A. Wilson
Sherman Fairchild Professor of Neuroscience
Director of Graduate Education for Brain and Cognitive Sciences

Structure-Function Relationships in Human Brain Development

by

Zeynep Mevhibe Saygin

Submitted to the Department of Brain and Cognitive Sciences

on June 25 2012, in partial fulfillment of the

requirements for the degree of

Doctor of Philosophy in Neuroscience

Abstract

The integration of anatomical, functional, and developmental approaches in cognitive neuroscience is essential for generating mechanistic explanations of brain function. In this thesis, I first establish a proof-of-principle that neuroanatomical connectivity, as measured with diffusion weighted imaging (DWI), can be used to calculate connectional fingerprints that are sufficient to delineate fine anatomical distinctions in the human brain (Chapter 2). Next, I describe the maturation of structural connectivity patterns by applying these connectional fingerprints to over a hundred participants ranging from five to thirty years of age, and show that these connectional patterns have different developmental trajectories (Chapter 3). I then illustrate how anatomical connections may shape (or in turn be shaped by) function and behavior, within the framework of reading ability and describe how white matter tract integrity may predict future acquisition of reading ability in children (Chapter 4). I conclude by summarizing how these experiments offer testable hypotheses of the maturation of structure and function. Studying the complex interplay between structure, function, and development will get us closer to understanding both the constraints present at birth, and the effect of experience, on the biological mechanisms underlying brain function.

Thesis Supervisors: John D. E. Gabrieli; Rebecca R. Saxe
Titles: Grover Hermann Professor in Health Sciences and Technology and Cognitive Neuroscience; Associate Professor of Cognitive Neuroscience

Contents

Acknowledgments

I am incredibly fortunate to have supportive mentors, John Gabrieli and Rebecca Saxe. John gave me the freedom to explore unfamiliar territory and encouraged me to focus on the ideas that most interested me. He is one of the kindest, yet sharpest, individuals I know, and I hope to provide the same level of encouragement, confidence, and critical advice to my own students one day. I am lucky to have yet another exceptional role model in Rebecca. She was willing to learn alongside me, while simultaneously teaching and providing me with direction. She was crucial in helping me develop my ideas and experiments, and afforded me with countless hours of motivation and inspiration. John and Rebecca have provided exceptional advising and have taught me how to better express myself scientifically. Through example, they also showed me how to be directed and confident, and to always strive to share and teach whenever possible.

I am also grateful to my other committee members, who have been extremely approachable and nurturing. Nancy Kanwisher is an exceptionally passionate scientist and teacher. Her comments and edits have been invaluable to the improvement of this thesis. I admire her precision and carefulness, and her work has inspired much of my scientific thinking and reasoning. I am extremely excited and looking forward to working with her in the future. Jean Augustinack has been integral in the amygdala segmentations and ex-vivo projects. I thank her for being open to new directions and for exuding an infectious respect towards neuroanatomy. I also look forward to continued collaboration with her.

I thank the each of the past and present members of the Gabrieli and Saxe labs, whose intellect and camaraderie have truly enriched my experience in graduate school. In particular, I was lucky to work closely with and learn greatly from several post-docs when I first started in the Gabrieli lab, including Elizabeth Redcay, Frida Polli, and Margaret Sheridan. I also received invaluable support and insight from my fellow graduate student Todd Thompson and research technicians Gretchen Reynolds and Sonny Sabhlok. I could not have survived these projects without each of you. I then had the pleasure to work with Dorit Kliemann, Elizabeth Norton, Kami Koldewyn, Marina Bedny, and Satra Ghosh, whose wisdom has proven indispensable to the present experiments and my graduate outlook in

general. A special shout-out to my formidable Basal Gangstas, Amy Finn, Rebecca Martin, and Margaret Sheridan, who are exuberant with academic curiosity, especially with regard to the basal ganglia, and whom I am delighted to have known, worked, and made delicious dinners with. I am also honored to have collaborated with the members of the Fischl lab, who took me in as one of their own, and I especially thank Allison Player, Anastasia Yendiki, Andre van der Kouwe, Bruce Fischl, Doug Greve, Lilla Zollei, and Martin Reuter, who were integral (and patient) in helping me get the first amygdala project off the ground. I look forward to continuing to work with many, if not all, of the brilliant individuals mentioned here.

None of this work would have been possible without my funding sources: the Presidential Graduate Fellowship, Advanced Multimodal Neuroimaging Training Program, Sheldon Razin Graduate Student Fellowship, and Poitras funding. I would also like to sincerely thank Denise Heintze for her endless dedication and support to me and all course 9 graduate students.

To my parents, Gülgün and Selim Saygin, two of the most important influences on my entire life: thank you for your endless support and for believing in me and my abilities without pause or question, and for encouraging me to always pursue my dream.

Finally, David Osher, my husband, best friend, and frequent collaborator, whose support and confidence in me is infinite and unwavering. He has been by my side through thick and thin; we share all our frustrations and disappointments, but we also share all the wonder and excitement of scientific discovery with each day. I have never met a person as brilliant, philosophically inclined, pragmatically sound, or as humble. We have learned everything together, and have grown substantially over graduate school, and I know that we will continue to do so. This thesis is dedicated to you.

Chapter 1

Introduction

"In the early sixties having begun to describe the physiology of cells in the adult (cat) visual cortex, David Hubel and I decided to investigate how the highly specific response properties of cortical cells emerged during postnatal development" Torsten Wiesel 1981.

Much like trying to understand any machine, deciphering the neural systems that give rise to human cognition and perception will involve reverse engineering. For example, to understand how a car works, one might first dissect the system into separate functional components such as pistons, wheels, or the carburetor; importantly, one next follows the cables and hoses to see what these components are connected with and how they come together to work in tandem. Neuroscientific research, especially human neuroimaging research, has made important advancements in identifying functional compartments in the brain (e.g. Kanwisher et al., 1997a,b; Saxe, Kanwisher et al. 2003; Epstein, Kanwisher et al., 1998; Kanwisher, Dilks et al. 2012). Now the focus of research can shift to understanding how these compartments interact with one another.

The integration of anatomical connections and functional responses is crucial in understanding how these regions work together to produce behavior. Fundamental discoveries in neuroscience have been guided by this concept. For example, Hubel and Wiesel's investigations[1] of primary visual cortex (V1) provided fundamental *descriptions* of the region's functional role, but descriptive accounts lack mechanistic substance; their subsequent *explanations* (**Figure 1**) of these phenomena employed models of connectivity which could produce the responses they had reported in V1. Hubel and Wiesel followed this work with another series of experiments, because they recognized that the mature working state of the brain is the product of development and plasticity.

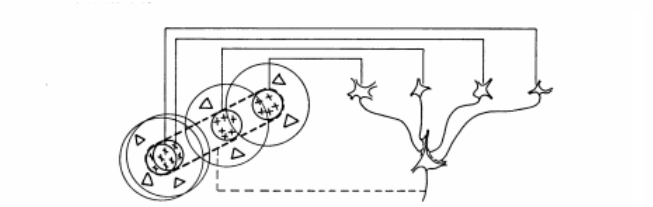

Figure 1. Connectionist model from Hubel and Wiesel, 1962. Original figure caption: "Possible scheme for explaining the organization of simple receptive fields. A large number of lateral geniculate cells, of which four are illustrated in the upper right in the figure, have receptive fields with 'on' centres arranged along a straight line on the retina. All of these project upon a single cortical cell, and the synapses are supposed to be excitatory. The receptive field of the cortical cell will then have an elongated 'on' centre indicated by the interrupted line in the receptive-field diagram to the left of the figure.

Hubel and Wiesel tested the possibility that early experience had a crucial role in shaping V1 responses. By recording the ocular preferences of V1 neurons in kittens reared with visual input from only one eye, the researchers discovered that early visual experience was crucial for normal development of binocular vision (Wiesel and Hubel 1965a,b). These studies illustrate the large influence that experience has in shaping this system. It is quite possible that more complex domains, such as language and reading, or socioemotional processing, are similarly shaped by experience. Studying the structural

[1] Hubel and Wiesel discovered that V1 neurons respond to moving gratings, rather than spots of light, which upstream neurons in both the retina and lateral geniculate nucleus (LGN) respond to. Hubel and Wiesel realized that there must be a transformation happening at the level of V1. They posited that the pattern of connectivity to V1 could allow the integration of neuronal responses and proposed a mechanism similar to center-surround mechanisms in the retina.

substrate of function in the developing brain will get us closer to understanding what constraints are present at birth and the effect of experience on the biological mechanisms underlying brain function.

In the human brain, methodological problems have prevented the establishment of such developmental principles of structural organization. Classic approaches in connectivity, such as histological tract-tracing have defied quantification. Further, it has been difficult to relate any such assessments of structural connectivity to functional measurements in the same individual. A method called diffusion-weighted imaging (DWI) offers a way to link structural connectivity estimates to functional activation in the brain (assessed by fMRI). Furthermore, DWI allows scientists to acquire structural information from children too young to perform fMRI experiments; structural data can be easily acquired from a cooperative child while he/she simply watches his/her favorite cartoon while in the MR scanner.

DWI is an MRI technique that measures the propensity of water to travel along myelinated axons, and can therefore be used to estimate brain connectivity *in vivo* (Basser, Mattiello et al. 1994; Behrens, Johansen-Berg et al. 2003a; Behrens, Woolrich et al. 2003b). These DW images can be acquired alongside fMRI data in the same individual. The acquisition method is similar to that of an Echo-Planar-Imaging (EPI) sequence (used for acquiring fMRI) but with the application of magnetic gradients varying in spatial direction. In a simplified sense, the concept of DWI is as follows: while pure water will diffuse randomly in all directions (isotropic), white matter tissue has fatty boundaries from myelinated axons, which will restrict the movement of water molecules. Water will move

along these axons and thus possess a biased direction of diffusion (anisotropic), which allows us to estimate the direction in which the fibers are oriented. Thus these DW images can be used to estimate a model per voxel and calculate the direction of greatest diffusion, and thus the most likely fiber orientation direction. Reconstructing the fiber tracts (tractography) can then be performed with further modeling by following these orientation directions from a seed voxel to any other voxel in the brain.

It is important to note that these methods can be influenced by many factors, ranging from image acquisition and quality, to post-hoc modeling. However, the DWI data presented in the following chapters are among the highest quality and analyzed using conservative algorithms (Behrens et al. 2003b). Also, the few studies that have compared the gold standard of histology to DWI have shown overall good correspondence (e.g. Peled, Berezovskii et al. 2005; Dauguet, Peled et al. 2007; Seehaus, Roebroeck et al. 2012).

Mechanistic explanations of human brain function can only be discovered by integrating structural and functional assessments (e.g. Saygin, Osher et al. 2012). Further, the role of early experience in shaping these mechanisms requires a developmental approach. In this thesis, I first establish a proof-of-principle that structural connectivity, as measured with DWI, can be used to calculate connectional patterns that are sufficient to delineate finer anatomical distinctions than previously possible (Chapter 2). These patterns of connectivity are specific to the resulting anatomical parcels and thus represent connectional fingerprints, or structural markers. I then describe the maturation of connectivity patterns by applying these structural markers to over a hundred participants ranging from five to thirty years of age, and show that some of these connectional patterns

have different developmental trajectories from the rest (Chapter 3). Lastly, I illustrate how structural connectivity may shape (or in turn be shaped by) function and behavior, within the framework of reading ability and describe how white matter tract integrity may predict future acquisition of reading in children (Chapter 4).

To establish the proof-of-principle, Chapter 2 focuses on the connectivity patterns of the amygdala. This brain region plays an important role in emotional and social functions, and its dysfunction has been associated with multiple neuropsychiatric disorders, including autism, anxiety, and depression. Although the amygdala is composed of multiple anatomically and functionally distinct nuclei, typical structural magnetic resonance imaging (MRI) sequences are unable to discern them. Thus, functional MRI (fMRI) studies typically average the BOLD response over the entire structure, which reveals some aspects of amygdala function as a whole but does not distinguish the separate roles of specific nuclei in humans. I propose a method to segment the human amygdala into its four major nucleus groups using only diffusion-weighted imaging and connectivity patterns derived mainly from animal studies. This new method is referred to as Tractography-based Segmentation, or TractSeg. The segmentations derived from TractSeg are topographically similar to their corresponding amygdaloid nuclei, and validated against a high-resolution scan in which the nucleic boundaries were visible. In addition, nucleus topography is consistent across subjects. TractSeg relies on short scan acquisitions and widely accessible software packages, making it attractive for use in healthy populations to explore normal amygdala nucleus function, as well as in clinical and perhaps pediatric populations. Finally, it paves the way for implementing this method in other anatomical regions which are also

composed of functional subunits that are difficult to distinguish with standard structural MRI.

Interestingly, when TractSeg is applied to the amygdalae of children, the algorithm fails to properly segment the nuclei, indicating that children possess relatively different connectivity patterns than adults. While there are no large developmental changes in the volume of the amygdala, functional differences do exist, as corroborated by behavioral and neuroimaging studies. Given previously reported whole-brain changes in white matter volume that occur through childhood, one possible basis for these functional differences could be the maturation of amygdalar connections with the rest of the brain. Using TractSeg, I test the hypothesis that the structural connectivity of this region changes with age (Chapter 3). I report that the reason the expressions of nucleus classification failed in young children is that amygdala connectivity is generally higher in children than in adults and that the specific connectivity patterns that drive this developmental change can be used to predict biological age. Further analyses reveal that these changes are specific to the basal and lateral nuclei of the amygdala and their connections with certain cortical and subcortical brain regions.

The next logical step would be to examine the functional ontogeny of the nuclei and their respective networks. However, the experimental stimuli used to test these functions will have to be graphic, startling, or fear-eliciting; the amygdala responds reliably to stimuli of the most extreme intensity, such as gruesome or terrifying scenes for negative valence and pornography for positive valence (Anderson and Sobel 2003; Canli, Zhao, et al. 2000). These stimuli are certainly inappropriate for children. Furthermore, it is difficult to assess

the amount of exposure to fearful stimuli that any individual might have had prior to participating in an experiment, regardless of age. On the other hand, a number of behavioral phenomena are much more controlled with respect to age, such as the acquisition of specific skills like reading. So, I turn to dyslexia and reading ability in the last chapter (Chapter 4) to study the development of a different type of structure-function relationship.

Developmental dyslexia has been associated with alterations in white matter organization but it is yet unknown whether these differences in structural connectivity are related to the cause of dyslexia, or instead are consequences of reading difficulty (e.g., less reading experience or compensatory brain organization). We scanned children at 5 years of age, much younger than previously reported, because at this age they have had little or no reading instruction. I show that differences in white matter integrity in the left arcuate fasciculus are already present in kindergarteners who are at risk for dyslexia due to poor phonological awareness. These results suggest a structural basis of risk for dyslexia that predates reading instruction. This finding illustrates one way that structure may constrain function and behavior, and the extent to which these structural constraints could be influenced by experience and maturation.

Chapter 5 summarizes these experiments and argues that they demonstrate principles of anatomical organization, function, and development in the human brain. I first discuss the benefits of establishing connectivity fingerprints of fine-grained human neuroanatomy (amygdala nuclei). I then propose possible functional implications of such connectivity fingerprints. Next, I describe the ontogeny of these fingerprints and offer

discrete and plausible biological mechanisms for these maturational changes, as well as the functional relevance of such mechanisms. I also specify why these experiments offer testable hypotheses of the maturation of structure and function. I conclude by discussing future directions that will further establish the ways in which specific structure-function relationships can arrive at a mature state through development and experience.

References

Anderson, A. K. and N. Sobel (2003). "Dissociating intensity from valence as sensory inputs to emotion." Neuron **39**(4): 581-583.

Basser, P. J., J. Mattiello, et al. (1994). "MR diffusion tensor spectroscopy and imaging." Biophysical journal **66**(1): 259-267.

Behrens, T. E., H. Johansen-Berg, et al. (2003a). "Non-invasive mapping of connections between human thalamus and cortex using diffusion imaging." Nature Neuroscience **6**(7): 750-7.

Behrens, T. E., M. W. Woolrich, et al. (2003b). "Characterization and propagation of uncertainty in diffusion-weighted MR imaging." Magn Reson Med **50**(5): 1077-88.

Canli, T., Z. Zhao, et al. (2000). "Event-related activation in the human amygdala associates with later memory for individual emotional experience." Journal of Neuroscience **20**(19).

Dauguet, J., S. Peled, et al. (2007). "Comparison of fiber tracts derived from in-vivo DTI tractography with 3D histological neural tract tracer reconstruction on a macaque brain." Neuroimage **37**(2): 530-8.

Epstein, R., & Kanwisher, N. (1998). "A cortical representation of the local visual environment." Nature, **392**(6676), 598-601.

Kanwisher, N. G., McDermott, J., & Chun, M. M. (1997a). The fusiform face area: A

module in human extrastriate cortex specialized for face perception. Journal of Neuroscience, **17**(11), 4302-4311.

Kanwisher, N., Woods, R. P., Iacoboni, M., & Mazziotta, J. C. (1997b). A locus in human extrastriate cortex for visual shape analysis. J Cogn Neurosci, **9**(1), 133-142.

Kanwisher, N., Dilks, D. (in press). "The Functional organization of the ventral visual pathway in humans." In Chalupa, L. & Werner, J. (Eds.), The New Visual Neurosciences.

Hubel, D.H., Wiesel, T.N. (1962). " Receptive fields, binocular interaction and functional architecture in the cat's visual cortex." J.Physiology, **160**(1): 106-154.2.

Peled, S., V. Berezovskii, et al. (2005). Histological validation of DTI using WGA-HRP in a macaque.

Saygin, Z. M., Osher, D. E., Koldewyn, K., Reynolds, G., Gabrieli, J. D. E., & Saxe, R. R. (2012). "Anatomical connectivity patterns predict face selectivity in the fusiform gyrus." Nature Neuroscience (15), 321-327.

Saxe, R., Kanwisher, N. (2003). "People thinking about thinking people. The role of the temporo-parietal junction in theory of mind." NeuroImage **19** (4): 1835–1842.

Seehaus, A. K., A. Roebroeck, et al. (2012). "Histological Validation of DW-MRI Tractography in Human Postmortem Tissue." Cerebral Cortex.

Wiesel TN, Hubel DH. (1965a). “Comparison of the effects of unilateral and bilateral eye closure on cortical unit responses in kittens”. J Neurophysiol **28**: 1029–1040.

Wiesel TN, Hubel DH. (1965b). “Extent of recovery from the effects of visual deprivation in kittens.” J Neurophysiol **28**: 1060–1072.

Wiesel, T. (1982). "The postnatal development of the visual cortex and the influence of environment (The 1981 Nobel Prize Lecture)." Stockholm: Nobel Foundation.

Chapter 2

Connectivity-based segmentation of human amygdala nuclei using probabilistic tractography[2]

The amygdala plays an important role in emotional and social functions, and amygdala dysfunction has been associated with multiple neuropsychiatric disorders, including autism, anxiety, and depression. Although the amygdala is composed of multiple anatomically and functionally distinct nuclei, typical structural magnetic resonance imaging (MRI) sequences are unable to discern them. Thus, functional MRI (fMRI) studies typically average the BOLD response over the entire structure, which reveals some aspects of amygdala function as a whole but does not distinguish the separate roles of specific nuclei in humans. We developed a method to segment the human amygdala into its four major nuclei using only diffusion-weighted imaging and connectivity patterns derived mainly from animal studies. We refer to this new method as Tractography-based Segmentation, or TractSeg. The segmentations derived from TractSeg were topographically similar to their corresponding amygdaloid nuclei, and were validated against a high-resolution scan in which the nucleic boundaries were visible. In addition, nuclei topography was consistent across subjects. TractSeg relies on short scan acquisitions and widely accessible software packages, making it attractive for use in healthy populations to explore normal amygdala nucleus function, as well as in clinical and pediatric populations. Finally, it paves the way for implementing this method in other anatomical regions which are also composed of functional subunits that are difficult to distinguish with standard structural MRI.

---

[2] Parts published as: Saygin Z.M.*, Osher D.E.*, Augustinack J., Fischl B., Gabrieli J.D.E. (2011). Connectivity-based segmentation of human amygdala nuclei using probabilistic tractography. Neuroimage, 56(3), 1353-1361.

2.1 Introduction

The amygdala is a complex structure composed of a heterogeneous group of nuclei and subnuclei, which are primarily defined by distinct cytoarchitectonics and differing connectivity patterns (Freese and Amaral, 2005, 2006, 2009; Alheid, 2003; Price et al., 1987; Aggleton, 2000; Gloor, 1972, 1978, 1997; McDonald, 1998). Although the names and boundaries of these nuclei remain disputed, they are commonly grouped into four main divisions: lateral (LA), basal and accessory basal (BA), medial and cortical (ME), and central (CE) (e.g. LeDoux, 1998). These structures are also functionally distinct. For example, LA is involved in learning new stimulus-affect associations (Johansen et al., 2010), whereas ME is involved in olfactory associations and sexual behavior (Lehman et al., 1980; Bian et al., 2008). These functions are likely determined by the afferent and efferent connectivity patterns to each region (LeDoux, 1996; Swanson and Petrovich, 1998; Pitkanen et al., 1997). For example, LA and BA are engaged in updating current stimulus value associations, primarily through connections with orbitofrontal regions (Baxter and Murray, 2002), whereas CE is believed to mediate behavioral responses to potentially harmful stimuli through its connectivity with hypothalamus, basal forebrain, and the brainstem (Kalin et al., 2004).

The distinct functions of the amygdala nucleus groups are not well-understood in the human brain, however, because the nuclei cannot be differentiated in standard magnetic resonance imaging. This is regrettable, because multiple studies suggest amygdalar involvement in psychopathology, such as mood (Phillips et al., 2003), anxiety (Rauch et al., 2003), and developmental disorders (Baron-Cohen et al., 2000). Some

attempts have been made to segment the amygdala, either manually through visual approximation based on a single-subject histological atlas (Etkin et al., 2004), or automatically by normalizing the subject's brain to a template brain and applying a thresholded probabilistic atlas (Amunts et al., 2005). The former approach is labor intensive and susceptible to human error, whereas the latter approach is prey to normalization errors. Further, the use of any atlas necessarily disregards individual differences in nucleic anatomy. Without an easily accessible and robust technique with which to compartmentalize the amygdala, it is difficult to elucidate the separate roles of the human amygdaloid nuclei, as well as the impact of individual differences in nucleus structure and function. Moreover, progress towards mechanistic theories of dysfunction and abnormal development will remain hindered until these structures can be explored *in vivo*.

Given the unique set of extrinsic connections for each nucleus, it may be possible to differentiate the distinct nuclei by their anatomic connectivity patterns. A metric of structural connectivity can be acquired non-invasively through diffusion weighted imaging (DWI), an MRI method that utilizes the propensity of water to travel along myelinated axons. Fibers can then be reconstructed using a variety of methods collectively termed tractography.

We adapted and extended methods that used probabilistic tractography (Behrens et al., 2003a) to divide each subject's set of amygdaloid voxels into logical subsets, using Boolean expressions. Boolean logic has several properties that make it potentially advantageous for segmenting regions with highly overlapping connectivity patterns such

as the amygdaloid nuclei. First, Boolean expressions can define precise combinations of connectivity patterns through specifically defined sets of unions, intersections, and negations. This should be an effective approach in disambiguating the similar connectivity profiles among amygdaloid nuclei. Second, we expected that this would be particularly useful when combining several smaller nuclei or subnuclei with distinct connectivity patterns. For example, LA is composed of dorsal, dorsal intermediate, ventral intermediate, and ventral subnuclei (Pitkanen and Amaral, 1998; Price et al., 1987), but these subdivisions are too small for typical scan resolutions and so are combined here for practical purposes. Boolean logic can easily combine connectivity patterns of these small subnuclei into a single unit. Finally, Boolean logic is especially appropriate when connectivity patterns are known *a priori* and are well-explored; a single expression can then be directly constructed from actual anatomical data.

Here we present a novel method, TractSeg (Tractography-based Segmentation), that localizes the four main nucleus groups in the living human amygdala (BA, LA, CE, and ME) using probabilistic tractography on DWI scans that take less than ten minutes to acquire. We hypothesized that it was possible to delineate subregions in the human amygdala based on connectivity patterns derived mainly from animal studies. To validate this method, we compared these subregions with the known topography of their corresponding nuclei, and tested how well they mapped on to the nucleic boundaries observable with a high-resolution scan. In addition, we assessed the across-subject consistency of TractSeg by measuring the spatial overlap between subjects' nuclei, in a reference frame produced by rigid-body rotation based on each subject's own amygdalae.

2.2 Methods

Subjects

Thirty-six subjects were recruited from the greater Boston area between the ages of 19 and 42 (mean age=25.7±0.2, 19 female). Subjects were screened for history of mental illness and were compensated at $30/hr. The diffusion sequences and anatomical sequences took approximately 20 minutes. The study was approved by the Massachusetts Institute of Technology and Massachusetts General Hospital ethics committees.

Acquisition

Diffusion-weighted data were acquired using echo planar imaging (64 slices, voxel size 2x2x2mm, 128x128 base resolution, diffusion weighting isotropically distributed along 60 directions, b-value 700s/mm^2) on a 3T Siemens scanner with a 32 channel head-coil (Reese et al., 2003). A high resolution (1mm^3) 3D magnetization-prepared rapid acquisition with gradient echo (MPRAGE) scan was also acquired on these subjects. An additional higher-resolution scan, which was optimized to differentiate amygdala nuclei in-vivo, was obtained on one of the subjects (dual-echo TE_0=5ms, TE_1=12ms, TR=20ms, 20^0 flip angle, 600μm x 600 μm x 600 μm, 8 runs registered and averaged). All analyses were performed on subject-specific anatomy, rather than extrapolation from a template brain.

Tractography

Automated cortical and subcortical parcellation was performed (Fischl et al., 2002, 2004) to define specific cortical and subcortical regions in each individual's T1 scan.

Automated segmentation results were reviewed for quality control, and were then registered to each individual's diffusion images, and used as the seed and target regions for fiber tracking. The resulting cortical and subcortical targets (including the amygdala) were then checked, and corrected for parcellation errors if necessary. The principal diffusion directions were calculated per voxel, and probabilistic diffusion tractography was carried out using FSL-FDT (Behrens et al., 2003b, 2007) with 25000 streamline samples in each seed voxel to create a connectivity distribution to each of the target regions, while avoiding a mask consisting of the ventricles.

Classification

In each subject, we calculated the connection probability (using FSL-FDT's probtrackX) from each amygdala voxel (seed) to all bilateral cortical and subcortical regions (targets), and normalized the distribution of probabilities for each seed voxel to [0,1] by dividing by the maximum probability. We then thresholded and binarized these results to exclude values below 0.1, such that every amygdaloid voxel contained a 0 or 1 for each target.

Since many of the targets are connected to more than one amygdaloid nucleus (as are nuclei connected to more than one target), we built four Boolean expressions describing the ipsilateral targets that putatively connect with four amygdala nuclei *a*) LA *b*) BA *c*) ME and *d*) CE. We derived these expressions from histological tracing studies of animal amygdalae, such that each expression reflects known connectivity patterns of the individual nuclei (**Table 1**). We then applied these expressions to the connectivity distribution of each amygdala voxel. Those that fit an expression were classified as

belonging to the corresponding nucleus, whereas voxels that did not match any expression remained unclassified.

Table 1. Definition of nucleus groups as based on summary of histological tracer studies in rats, nonhuman primates, and humans.

Target combinations	Putative nucleus
~(Superior parietal **|** Post-central[1-4] **|** Medial orbitofrontal[1,2,5] **|** Lateral occipital **|** Pericalcarine **|** Cuneus[6]) **&** (Temporal pole **|** Fusiform **|** Lateral orbitofrontal **&** (Superior temporal **|** Inferior Temporal[1-3,7-9,26])))	Lateral
(Parahippocampus[6] **&** (Hippocampus[15,16] **|** Rostral anterior cingulate[6,17] **|** Lateral orbitofrontal **|** Medial orbitofrontal[18,2,3,5] **|** Caudal middle-frontal **|** Lateral occipital **|** Pericalcarine **|** Cuneus **|** Lingual[6,19,20, 26])) **|** (Insula **&** (Accumbens **|** Superior frontal[6,21-23]))	Basal
~(Brain Stem[10,11] **&** Ventral Diencephalon[6,12,13] **&** Thalamus Proper[14]) **&** (Ventral Diencephalon[24,25] **&** (Striatum[5] **|** Hippocampus[15,16]))	Medial
Brain Stem[10,11] **&** Ventral Diencephalon[6,12,13] **&** Thalamus Proper[14]	Central

Table References

1. *(Aggleton et al., 1980)*
2. *(Stefanacci and Amaral, 2000)*
3. *(Stefanacci and Amaral, 2002)*
4. *(Turner et al., 1980)*
5. *(Gloor, 1994)*
6. *(Amaral and Price, 1984)*
7. *(Kosmal et al., 1997)*
8. *(Yukie, 2002)*
9. *(Bachevalier et al., 1997)*
10. *(Price and Amaral, 1981)*
11. *(Price, 1981)*
12. *(Amaral et al., 1982)*
13. *(Mehler, 1980)*
14. *(Amaral et al., 1992)*
15. *(Aggleton, 1986)*
16. *(Amaral, 1986)*
17. *(Vogt and Pandya, 1987)*
18. *(Carmichael and Price, 1995)*
19. *(Amaral et al., 2003)*
20. *(Freese and Amaral, 2005)*
21. *(Barbas and De Olmos, 1990)*
22. *(Ghashghaei and Barbas, 2002)*
23. *(Russchen et al., 1985)*
24. *(Price, 1986)*
25. *(Price et al., 1987)*
26. *(Herzog and Van Hoesen, 1976)*

Legend

~ NOT **|** OR **&** AND

For example, the LA is the primary recipient of high-level sensory input, mainly from anterior temporal regions, and does *not* connect with lower-level visual regions; it also receives specific, but sparse, input from the lateral orbitofrontal cortex, but *not* from medial orbitofrontal cortex. Moreover, there is little evidence of parietal connectivity with the amygdala in general, and specifically none with LA. In order to encapsulate this connectivity pattern in a single expression, we began by negating any voxel that connects with parietal, occipital, or medial orbitofrontal cortices. The LA was defined as the intersection between the remaining subset of voxels and those that connect with anterior temporal cortices, namely temporal pole or fusiform gyrus, or lateral orbitofrontal cortex when also accompanied by connections with other anterior temporal cortices such as the inferior or superior temporal gyri, since BA also connects with lOFC. The three other expressions were also constructed in a similar manner to reflect specific connectivity patterns. The BA projects to all components of the ventral visual system and is reciprocally connected with frontal cortices, mainly mOFC and lOFC. In addition, it is also heavily connected with the hippocampus and related structures. The ME and CE are both highly connected with midbrain targets, but are distinct in their connections to brainstem, in addition to other targets. We therefore used the intersection of ventral diencephalon with the union of caudate and hippocampus to reflect ME connectivity, whereas CE connectivity was characterized by the brainstem, thalamus, and ventral diencephalon targets.

The resulting images were spatially smoothed per nucleus in 3-dimensions, based on the number of neighboring voxels of the same nucleus. Voxels with 6 or more neighbors were classified as the nucleus in question. In order to retain mutual exclusivity between nuclei, any overlapping voxels were classified as belonging to the smaller nucleus. This

was implemented in order to preserve boundaries between the nuclei while overcoming the inherent problems of thresholding by number of neighbors: smaller nuclei are more prone to lose voxels, while larger ones are more prone to gain voxels. In the case of no voxels surviving the threshold (which was infrequent: left central in one subject, left medial in another subject, and right central in a third subject), the original un-smoothed nucleus was used. They were then transformed from diffusion space back into each subject's anatomical coordinates, interpolated based on nearest neighbors, and overlaid on their anatomical MPRAGE scan for figures and quantitative analyses.

Comparison to manual segmentation

We optimized and acquired an additional high-resolution anatomical scan from one subject (see Acquisition). These high-resolution images were manually labeled based on visible boundaries between the four nuclei, and compared to the segmentation derived from tractography. Both the manual and tractographic segmentation images were registered to this subject's MPRAGE scan (down-sampled from 600um to 1mm and up-sampled from 2mm to 1mm respectively). Performance of the tractographic segmentations was assessed by the voxel-by-voxel correspondence between these two images. The accuracy for each nucleus was measured as the proportion of matching voxels in both segmentations. We also calculated d' for each nucleus in order to penalize false positives:

$$d' = norminv(hit\ rate) - norminv(false\ alarm\ rate)$$

where norminv(x) is the inverse of the cumulative Gaussian distribution.

Measures of consistency between subjects

In order to compare the outcome of the connectivity-based segmentation between subjects and still preserve subject-specific anatomy (keeping the images in native-space rather than in normalized-space), we rotated the amygdalae of each subject along an axis drawn from the center-of-masses of the amygdala and the fourth ventricle, correcting for inter-subject differences in pitch (yaw and roll were consistent across subjects). After correcting for head rotation, we placed each amygdala into a common reference frame (with each subject's amygdala centroid at the origin) by mean-shifting (subtracting the rotated coordinates from the amygdala center-of-mass). A conventional whole-brain approach would not have been practical or informative for comparing subjects or generating a probability map due to low cross-subject alignment of the entire amygdala; when we aligned subjects to the template T1 image provided by SPM8, we found that only 57.58% of the subjects were consistent in the spatial location of the right amygdala, and 60.61% for the left (as compared to our method of alignment for which there was a 97.06% overlap for the right amygdala, and 100% for the left).

Each subject was then iteratively compared with every other subject, and both accuracy and d' were calculated per subject as the average overlap across the other subjects. We also calculated the mean volumes per nucleus across the subjects, and performed a two-sample Student's t-test across hemispheres. A cut-off of $p \leq 0.0125$ (Bonferroni corrected for multiple comparisons) was used for determining the significance of these tests.

We also generated a probability atlas (**Figure 4**) of the amygdaloid nuclei by aligning subjects' amygdalae as above, and calculating the proportion of subjects that share nucleus classification for each voxel. For the sake of visualization, **Figure 4** displays the atlas thresholded at 15/35 subjects.

2.3 Results

We defined four Boolean expressions that correspond with known connectivity patterns of the four major nucleus groups of the amygdala: LA, BA, CE, and ME (**Table 1**). The combination of target regions for LA defined the most ventrolateral subregion of the amygdala (as shown on an example subject, **Figure 1b-c)**. This was present along the full rostrocaudal extent **(Figure 1a)** of the amygdala, which is morphologically and spatially characteristic of LA (Gloor, 1997; Aggleton, 2000; Freese and Amaral, 2009). A similar, but distinct, pattern of connectivity (see Methods and **Table 1**) identified a more ventral amygdaloid region immediately medial to the LA, corresponding to the known location of the BA (Gloor, 1997; Aggleton, 2000; Freese and Amaral, 2009) **(Figure 1a-c)**. These two subregions were the largest of the tractographic classification, and indeed are the largest nuclei of the amygdala. The third expression defined an oblique subregion of the dorsomedial amygdala, a distinguishing feature of the ME **(Figure 1a-c)**, whereas the last expression classified voxels that were present in the dorsal amygdala and appeared in the caudal-most region, much like the CE (**Figure 1a**). The four nuclei were also comparable between hemispheres **(Figure 1a-b)**.

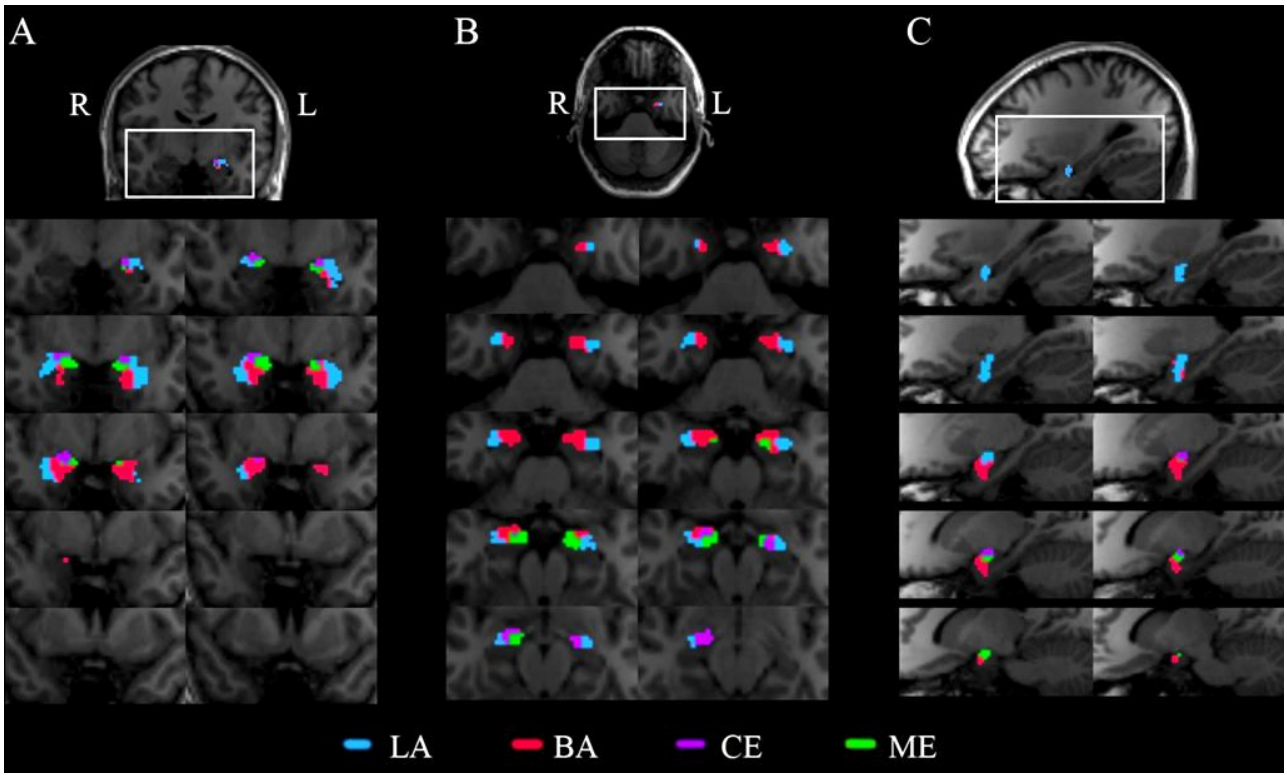

Figure 1 | Tractographic segmentation in an example subject. Right- and left-amygdala tractographic segmentation are resampled into anatomical coordinates, and overlaid on the same subject's MPRAGE images. Nuclei are color-coded as: BA (red), LA (blue), ME (green), CE (purple). **a,** Coronal sections from posterior to anterior extents of the amygdalae demonstrate the comparable segmentations for both hemispheres, and also illustrate that the LA and BA occupy the most rostral extents, while CE and ME appear more caudally. **b,** Axial sections from inferior to superior further describe the nuclei, where LA and BA are more ventral than CE or ME. **c,** Right sagittal sections from lateral to medial show the most lateral (LA) and medial (ME) nuclei in relation to the other nuclei.

High-resolution validation

In order to visualize the boundaries between the nuclei, we acquired an additional high-resolution anatomical scan from one subject (**Figure 2a)**. This scan, averaged over 8 runs totaling approximately two hours, gave us the resolution and contrast-to-noise ratio (CNR) needed to visualize the boundaries between the nuclei *in vivo*. These images were manually labeled to segment the amygdala into the 4 nuclei **(Figure 2b),** and compared to the connectivity-based segmentation based on the ten-minute diffusion-weighted sequence (**Figure 2c)** in the same subject. The size, shape, and location of the LA, BA, CE, and ME were markedly similar between the manually-labeled amygdala and the tractographic segmentation. Since both manual and tractographic segmentation were performed on the same individual, we were able to overlay and directly compare them. For each nucleus, we calculated accuracy as the proportion of matching voxels, and d' as the difference between standardized hit rates and false alarm rates, wherein values of 0 or <0 imply an overlap at or worse than chance, and d'≥1 indicating high sensitivity. The tractographic segmentation was very similar to the manual segmentation, with high accuracy rates in both hemispheres for the LA (R:0.86; L:0.71), BA (R:0.80; L:0.66), CE (R:0.89; L:0.85), ME (R:0.93; L:0.95) and high d' values LA (R:2.13; L:1.27), BA (R:1.76; L:1.19), CE (R:1.16; L:2.40), ME (R:2.30; L:2.14).

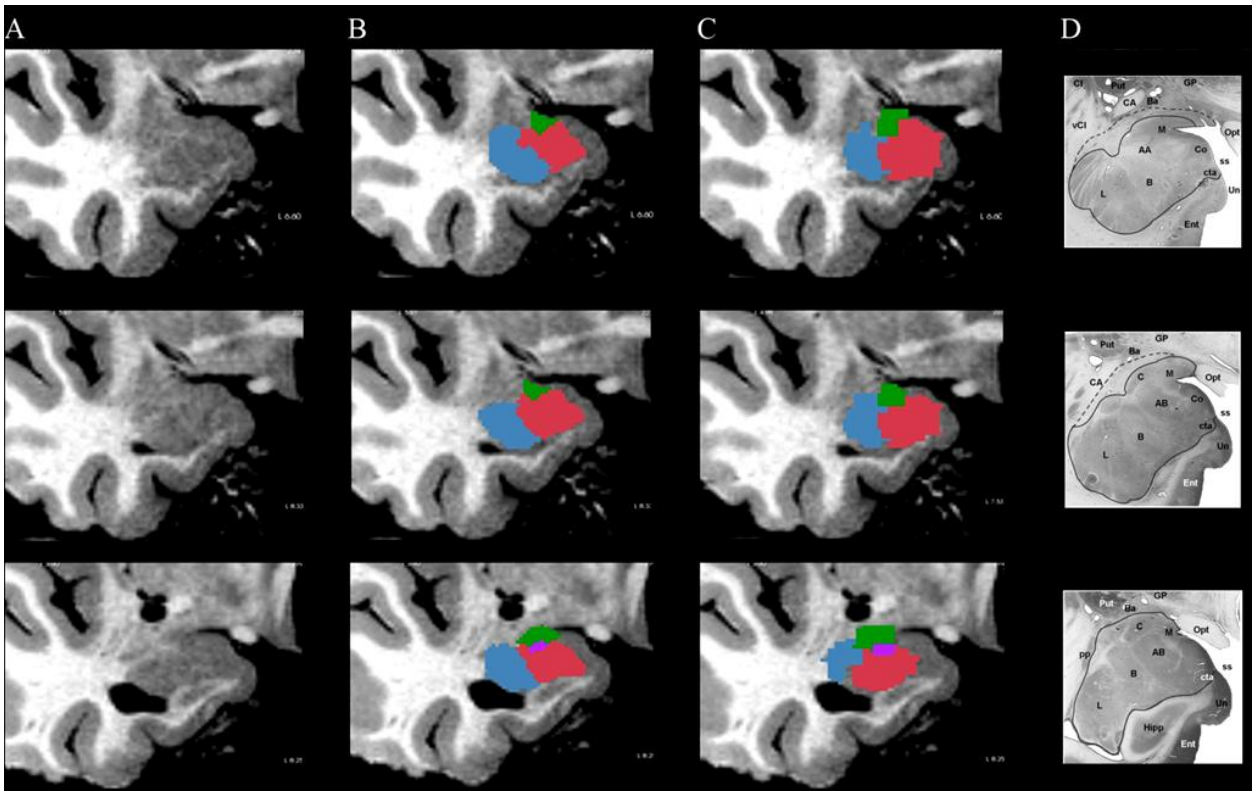

Figure 2 | Manual vs. tractographic segmentation. a, Coronal images of the right amygdala from a high-resolution scan (dual-echo 20° flip angle TE0 / TE1 / TR = 5ms/ 12ms/ 20ms 600μm isotropic) averaged over 8 runs. **b,** Boundaries visible from this scan were used to manually segment the amygdala into four nuclei, color-coded as in Figure1. **c,** Tractographic segmentation on the same individual was registered and overlaid on the same coronal slices as Figure 2a and b. The nuclei are visually similar to those based on a high-resolution scan, as well as to **d,** a coronal section based on a histological specimen of the human amygdala (Gloor, 1997).

Consistency across individuals

These subregions were also consistent in size, shape, and location across an additional 35 subjects, with lateral and basal occupying the largest volumes, central and medial the smallest (**Table 2**), and no between-hemisphere differences (LA: p=0.89; BA: p=0.24; CE: p=0.02; ME: p=0.34). We placed each subject's amygdala into a common reference frame via rigid body rotation, free of any spatial warping (see Methods). We were then able to visualize the consistency of nucleic location in three dimensions across individuals in both the right and left amygdalae **(Figure 3a).**

Table 2. Nucleus volumes in proportion to the whole amygdala across subjects.

	Lateral	**Basal**	**Central**	**Medial**
Left	0.40±0.03	0.32±0.02	0.16±0.01	0.12±0.02
Right	0.40±0.02	0.35±0.02	0.11±0.01	0.14±0.02

Values are reported in mean ± standard error.

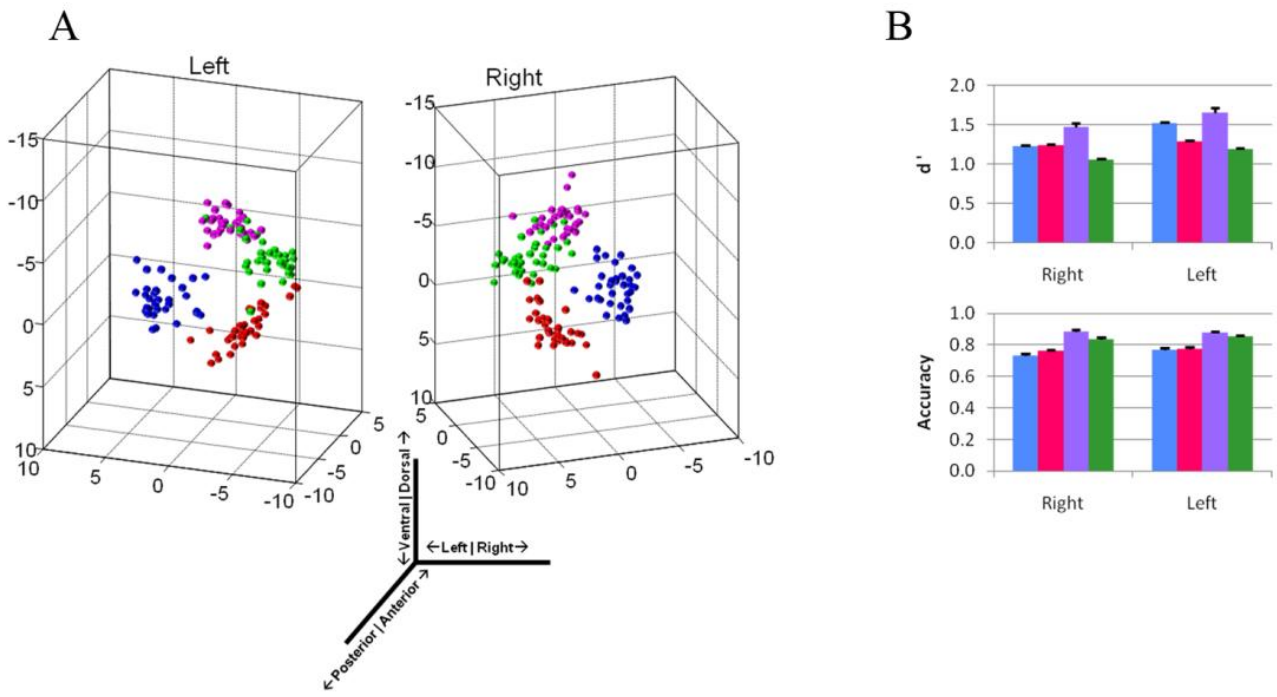

Figure 3 | Overlap of tractographic segmentation-based nuclei between subjects. a, Resulting centroid locations, after alignment (see methods), of the segmented nuclei are plotted from 35 subjects, demonstrating the similarity of nucleus location, in three dimensions. Nuclei are color-coded as in Figure 1. **b,** Right- and left-amygdala tractographic segmentation was consistent among 35 subjects, as indicated by high d' and accuracy values.

Accuracy and d' measures of overlap between subjects were calculated by iteratively using each subject as a reference in comparison to every other subject. As observed qualitatively, the degree of overlap was high across subjects for nuclei in both hemispheres, with high average accuracy rates **(Figure 3b)**: LA (R:0.73±0.01; L:0.77±0.01), BA (R:0.76±0.01; L:0.78±0.01), CE (R:0.89±0.01; L:0.88±0.01), ME (R:0.84±0.01;

L:0.85±0.01) and high average d' values: LA (R:1.23±0.05; L:1.52±0.06), BA (R:1.25±0.05; L:1.29±0.06), CE (R:1.47±0.05; L:1.66±0.05), ME (R:1.06±0.06; L:1.19±0.05). We used these amygdala subdivisions from our 35 subjects to generate a population-based atlas of the human amygdala, thresholded by overlap of at least 15 out of 35 subjects (**Figure 4**).

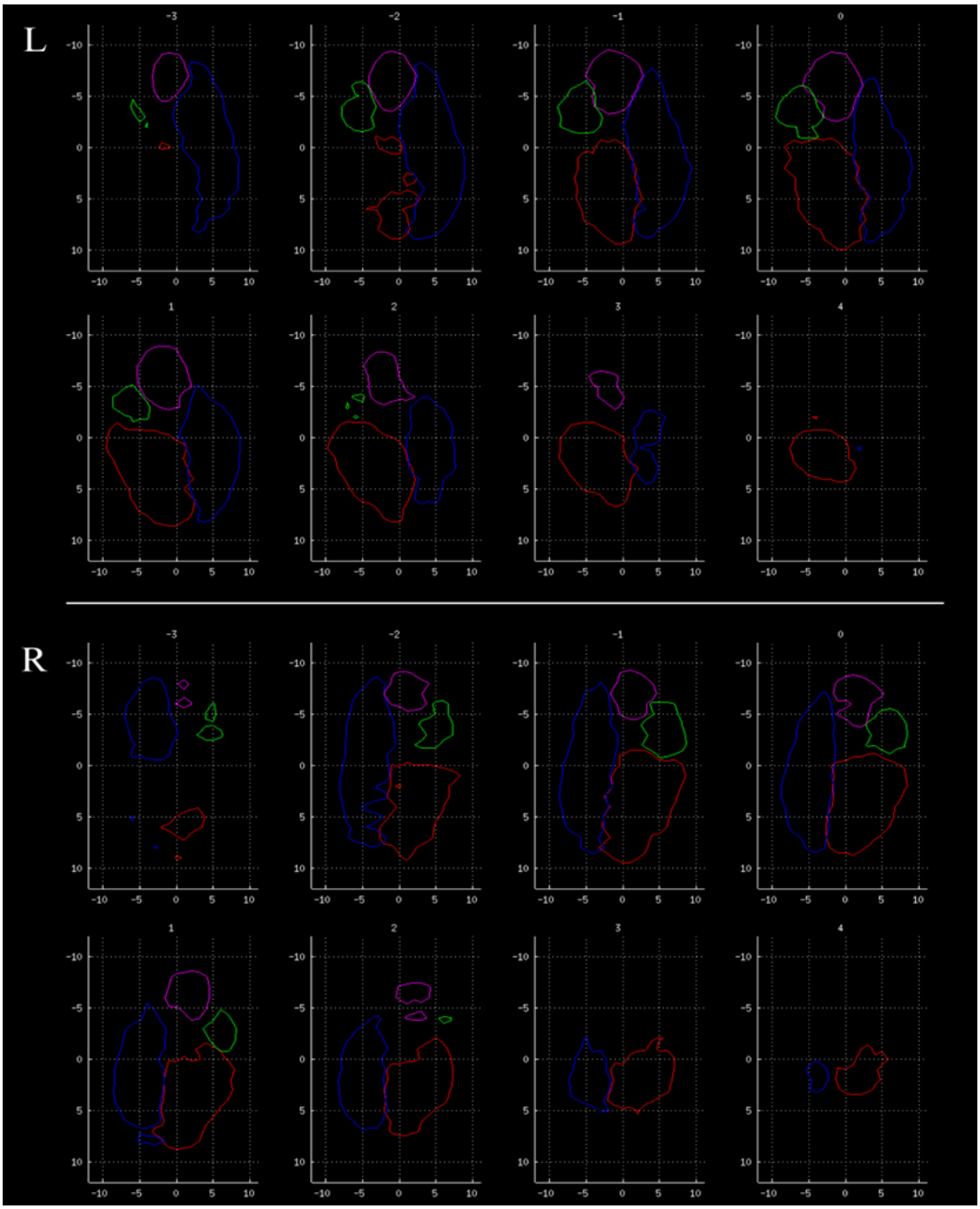

Figure 4 | Amygdala tractographic segmentation atlas. Coronal slices through the population's left (top panels) and right (bottom panels) amygdalae, from posterior to anterior, in rotated space. The edges of the group probability maps, thresholded at >= 15/35 subjects, are shown for each subregion (color-coded as in Figure 1). Units are in millimeters, and with respect to the amygdala centroid. The reference point for rotation (4th ventricle) is posterior and normal to the plane for all subjects.

2.4 Discussion

By exploiting the differential connectivity patterns of four amygdaloid nuclei, we generated logical statements that anatomically define four subregions in the amygdala. These expressions were based on connectivity patterns from non-human amygdalae, since there are few human tracer studies. Nonetheless, when these expressions were applied to tractographic reconstructions of the human amygdala, they generated spatially-distinct clusters that map well to their known locations. These subregions were spatially consistent across individuals, and were validated by a high-resolution image in one subject.

To the best of our knowledge, this is the first time that the amygdala has been non-invasively segmented into four putative nucleus groups based on structural connectivity patterns. Previous research used other methods, such as visual approximation to distinguish the dorsal vs. ventral amygdala (Etkin et al., 2004; Dolan, 2002, 2007; Dolan and Vuilleumier, 2003; Dolan et al., 2001, 2006) and posit functional roles for these subregions with fMRI, which can be further explored now at a single-subject level and with more subdivisions with which to predict and test models of amygdalar function. Fiber orientations (based on DWI scans) within the amygdala have been used to divide the structure into two subregions, centromedial and basolateral (Solano-Castiella et al., 2010). However, this method, like others before it, performed analyses on images normalized to a template brain, and were also restricted to two subdivisions. Visual approximation or normalization methods may be susceptible to errors which the current method circumvents. We used native-space analyses (Fischl et al., 2008) to generate target regions which were specific to individuals' anatomy, and performed all subsequent analyses in

native-space as well, such that the resulting amygdala subdivisions were also unique to the individual's own anatomy.

Native-space analyses better accommodate individual variation in subcortical volume (Di Martino et al., 2008; Pujol et al., 2010), and are thus best-suited for volumetric analyses and studies of clinical populations that have smaller or larger average amygdala volumes (e.g. Nacewicz et al., 2006; Brambilla et al., 2003; Chance et al., 2002). The current method could be implemented to explore differences in amygdaloid nucleus volumes and their relative contributions to the size of the whole amygdala. Furthermore, volumetric differences between populations, elucidated via TractSeg, could indeed be due to either nucleic variation or to connectivity differences between populations. This can be further explored by applying the probability atlas to the pathological population, and analyzing connectivity differences between the atlas-based segmentation and the subject-specific TractSeg-based segmentation. Additionally, future studies can investigate the relative contribution of connectivity versus actual amygdala subdivision differences by generating a database of nucleus volumes (based on histology and/or high-resolution imaging) in order to probe normal variations, and relate them to connectivity differences.

We also extended other efforts to segment the amygdala or other gray matter structures through connectivity by validating the connectivity-based subdivisions using a high-resolution structural scan, similar to a previous approach for localizing lateral geniculate bodies (Devlin et al., 2006). High-resolution scans averaged across multiple runs, such as the one developed for the purposes of this study, allow for dramatically better visualization than standard resolution images. However they are currently too long to be

commonly used in conjunction with other types of scans (such as functional MRI) and too strenuous for many subjects who cannot remain motionless throughout the scan; in our case, the high-resolution image took two hours to acquire. Such long scan durations are especially impractical for clinical and developmental applications. The present study used a DWI scan lasting less than ten minutes to segment the amygdala, and produced results that converged substantially with those of the optimized high-resolution acquisition.

Although we employed many of the basic principles and pre-processing steps of pioneering probabilistic tractographic studies, e.g. (Behrens et al., 2003a), our use of native-space analyses (discussed above) and Boolean logic extends these in ways that will facilitate future research at the single-subject level. This method can be applied to not only the amygdala, but to any gray matter structure. Furthermore, it is particularly effective because it allows for a combination of target regions and thus can be robust across individuals and noisy MR signals. These Boolean expressions can disambiguate the highly overlapping patterns of connectivity among gray matter nuclei with specifically defined sets of unions, intersections, and negations. It is particularly appropriate when connectivity patterns are known *a priori* in order to construct expressions that should theoretically define the nuclei in question. Future methods might also benefit from logical solutions that can handle continuous probabilities, as opposed to binarization, such as fuzzy logic, e.g. (McNeill and Freiberger, 1993).

One possible limitation of DWI in general is that the polarity of connections is unknown; future studies employing this method should keep this in consideration when building the sets of connectivity profiles. Also, since all cortical and subcortical regions

were used to create target regions and connectivity distributions to the amygdala, whole-brain coverage during DWI acquisition is necessary to use this method.

We suggest that this method has applications in exploring the functions of distinct nuclei, exploring structural and functional networks, and can be used to segment other gray matter regions. The regions-of-interest (ROIs) generated from this method (which remain in native space and are true to the individual's own anatomy in shape, size, and location) can be used as independently localized ROIs for fMRI analyses. This could be useful in elucidating the specific roles of distinct nuclei within the human amygdala, both in healthy controls, and in clinical populations. By expanding the seed region to encompass a larger region than what is typically defined as the amygdala, TractSeg can also be used to explore specific hypotheses of the function and structural organization of the extended amygdala (Cassell et al., 1999). Furthermore, the nuclei can be used as seed regions for functional connectivity analyses, and thus for exploring differences in functional networks between populations or across development. The nuclei might also be definable by these Boolean expressions but from functional rather than structural connectivity. This will broaden our understanding of the similarities or differences of structural vs. functional networks.

2.5 References

Aggleton, J. P. (1986) A description of the amygdalo-hippocampal interconnections in the macaque monkey. *Exp Brain Res,* 64**,** 515-26.

Aggleton, J. P., Burton, M. J. & Passingham, R. E. (1980) Cortical and subcortical afferents to the amygdala of the rhesus monkey (Macaca mulatta). *Brain Res,* 190**,** 347-68.

Aggleton, J. P. E. (2000) *The Amygdala,* Oxford, United Kingdom, Oxford University Press.

Alheid, G. F. (2003) Extended amygdala and basal forebrain. *Ann N Y Acad Sci,* 985**,** 185-205.

Amaral, D. G. (1986) Amygdalohippocampal and amygdalocortical projections in the primate brain. *Adv Exp Med Biol,* 203**,** 3-17.

Amaral, D. G., Behniea, H. & Kelly, J. L. (2003) Topographic organization of projections from the amygdala to the visual cortex in the macaque monkey. *Neuroscience,* 118**,** 1099-120.

Amaral, D. G. & Price, J. L. (1984) Amygdalo-cortical projections in the monkey (Macaca fascicularis). *J Comp Neurol,* 230**,** 465-96.

Amaral, D. G., Price, J. L., Pitkanen, A. & Carmichael, S. T. (1992) Anatomical organization of the primate amygdaloid complex. IN AGGLETON, J. P. (Ed.) *The Amygdala. Neurobiological Aspects of Emotion, Memory, and Mental Dysfunction.* New York, Wiley-Liss.

Amaral, D. G., Veazey, R. B. & Cowan, W. M. (1982) Some observations on hypothalamo-amygdaloid connections in the monkey. *Brain Res,* 252**,** 13-27.

Amunts, K., Kedo, O., Kindler, M., Pieperhoff, P., Mohlberg, H., Shah, N. J., Habel, U., Schneider, F. & Zilles, K. (2005) Cytoarchitectonic mapping of the human amygdala, hippocampal region and entorhinal cortex: intersubject variability and probability maps. *Anat Embryol (Berl),* 210**,** 343-52.

Bachevalier, J., Meunier, M., Lu, M. X. & Ungerleider, L. G. (1997) Thalamic and temporal cortex input to medial prefrontal cortex in rhesus monkeys. *Exp Brain Res,* 115**,** 430-44.

Barbas, H. & De Olmos, J. (1990) Projections from the amygdala to basoventral and mediodorsal prefrontal regions in the rhesus monkey. *J Comp Neurol,* 300**,** 549-71.

Baron-Cohen, S., Ring, H. A., Bullmore, E. T., Wheelwright, S., Ashwin, C. & Williams, S. C. (2000) The amygdala theory of autism. *Neurosci Biobehav Rev,* 24**,** 355-64.

Baxter, M. G. & Murray, E. A. (2002) The amygdala and reward. *Nat Rev Neurosci,* 3**,** 563-73.

Behrens, T. E., Berg, H. J., Jbabdi, S., Rushworth, M. F. & Woolrich, M. W. (2007) Probabilistic diffusion tractography with multiple fibre orientations: What can we gain? *Neuroimage,* 34**,** 144-55.

Behrens, T. E., Johansen-Berg, H., Woolrich, M. W., Smith, S. M., Wheeler-Kingshott, C. A., Boulby, P.., Barker, G.., Sillery, E., Sheehan, K., Ciccarelli, O., Thompson, A. J., Brady, J.

M. & Matthews, P. M. (2003a) Non-invasive mapping of connections between human thalamus and cortex using diffusion imaging. *Nat Neurosci,* 6**,** 750-7.

Behrens, T. E., Woolrich, M. W., Jenkinson, M., Johansen-Berg, H., Nunes, R. G., Clare, S., Matthews, P. M., Brady, J. M. & Smith, S. M. (2003b) Characterization and propagation of uncertainty in diffusion-weighted MR imaging. *Magn Reson Med,* 50**,** 1077-88.

Bian, X., Yanagawa, Y., Chen, W. R. & Luo, M. (2008) Cortical-like functional organization of the pheromone-processing circuits in the medial amygdala. *J Neurophysiol,* 99**,** 77-86.

Brambilla, P., Hardan, A., Di Nemi, S. U., Perez, J., Soares, J. C. & Barale, F. (2003) Brain anatomy and development in autism: review of structural MRI studies. *Brain Res Bull,* 61**,** 557-69.

Carmichael, S. T. & Price, J. L. (1995) Limbic connections of the orbital and medial prefrontal cortex in macaque monkeys. *J Comp Neurol,* 363**,** 615-641.

Cassell, M. D., Freedman, L. J. & Shi, C. (1999) The intrinsic organization of the central extended amygdala. *Ann N Y Acad Sci,* 877**,** 217-41.

Chance, S. A., Esiri, M. M. & Crow, T. J. (2002) Amygdala volume in schizophrenia: post-mortem study and review of magnetic resonance imaging findings. *Br J Psychiatry,* 180**,** 331-8.

Devlin, J. T., Sillery, E. L., Hall, D. A., Hobden, P., Behrens, T. E. J., Nunes, R. G., Clare, S., Matthews, P. M., Moore, D. R., And Johansen-Berg, H. (2006) Reliable identification of the auditory thalamus using multi-modal structural analyses. *Neuroimage,* 30(4), 1112-1120.

Di Martino, A., Scheres, A., Margulies, D. S., Kelly, A. M., Uddin, L. Q., Shehzad, Z., Biswal, B., Walters, J. R., Castellanos, F. X. & Milham, M. P. (2008) Functional connectivity of human striatum: a resting state FMRI study. *Cereb Cortex,* 18**,** 2735-47.

Dolan, R. J. (2002) Emotion, cognition, and behavior. *Science,* 298**,** 1191-4.

Dolan, R. J. (2007) The human amygdala and orbital prefrontal cortex in behavioural regulation. *Philos Trans R Soc Lond B Biol Sci,* 362**,** 787-99.

Dolan, R. J., Heinze, H. J., Hurlemann, R. & Hinrichs, H. (2006) Magnetoencephalography (MEG) determined temporal modulation of visual and auditory sensory processing in the context of classical conditioning to faces. *Neuroimage,* 32**,** 778-89.

Dolan, R. J., Morris, J. S. & De Gelder, B. (2001) Crossmodal binding of fear in voice and face. *Proc Natl Acad Sci U S A,* 98**,** 10006-10.

Dolan, R. J. & Vuilleumier, P. (2003) Amygdala automaticity in emotional processing. *Ann N Y Acad Sci,* 985**,** 348-55.

Etkin, A., Klemenhagen, K. C., Dudman, J. T., Rogan, M. T., Hen, R., Kandel, E. R. & Hirsch, J. (2004) Individual differences in trait anxiety predict the response of the basolateral amygdala to unconsciously processed fearful faces. *Neuron,* 44**,** 1043-55.

Fischl, B., Rajendran, N., Busa, E., Augustinack, J., Hinds, O., Yeo, B. T., Mohlberg, H., Amunts, K. & Zilles, K. (2008) Cortical folding patterns and predicting cytoarchitecture. *Cereb Cortex,* 18**,** 1973-80.

Fischl, B., Salat, D. H., Busa, E., Albert, M., Dieterich, M., Haselgrove, C., Van Der Kouwe, A., Killiany, R., Kennedy, D., Klaveness, S., Montillo, A., Makris, N., Rosen, B. & Dale, A. M. (2002) Whole brain segmentation: automated labeling of neuroanatomical structures in the human brain. *Neuron,* 33**,** 341-55.

Fischl, B., Van Der Kouwe, A., Destrieux, C., Halgren, E., Segonne, F., Salat, D. H., Busa, E., Seidman, L. J., Goldstein, J., Kennedy, D., Caviness, V., Makris, N., Rosen, B. & Dale, A. M. (2004) Automatically parcellating the human cerebral cortex. *Cereb Cortex,* 14**,** 11-22.

Freese, J. L. & Amaral, D. G. (2005) The organization of projections from the amygdala to visual cortical areas TE and V1 in the macaque monkey. *J Comp Neurol,* 486**,** 295-317.

Freese, J. L. & Amaral, D. G. (2006) Synaptic organization of projections from the amygdala to visual cortical areas TE and V1 in the macaque monkey. *J Comp Neurol,* 496**,** 655-67.

Freese, J. L. & Amaral, D. G. (2009) Neuroanatomy Of The Primate Amygdala. In Whalen, P. J. & Phelps, E. A. (Eds.) *The Human Amygdala.* New York, The Guilford Press.

Ghashghaei, H. T. & Barbas, H. (2002) Pathways for emotion: interactions of prefrontal and anterior temporal pathways in the amygdala of the rhesus monkey. *Neuroscience,* 115**,** 1261-79.

Gloor, P. (1972) Temporal lobe epilepsy: its possible contribution to the understanding of the functional significance of the amygdala and of its interaction with neocortical-temporal mechanisms. IN ELEFTHERION, B. E. (Ed.) *The Neurobiology of the Amygdala.* New York, Plenum Press.

Gloor, P. (1978) Inputs and outputs of the amygdala: what the amygdala is trying to tell the rest of the brain. IN LIVINGSTON, K. E. & HORNIKIEWICZ, O. (Eds.) *Limbic Mechanisms. The Continuing Evolution of the Limbic System Concept.* New York and London, Plenum Press.

Gloor, P. (1994) Mesial temporal lobe structures. IN SHORVON, S. D., FISH, D. R., ANDERMANN, F., BYDDER, G. M. & STEFAN, H. (Eds.) *Magnetic Resonance Scanning and Epilepsy.* New York/London, Plenum Press.

Gloor, P. (1997) *The Temporal Lobe and Limbic System,* New York, New York, Oxford University Press, Inc.

Herzog, A.G., Van Hoesen G.W. (1976) Temporal neocortical afferent connections to the amygdala in the rhesus monkey. *Brain Res,* 115(1), 57-69.

Johansen, J. P., Hamanaka, H., Monfils, M. H., Behnia, R., Deisseroth, K., Blair, H. T. & Ledoux, J. E. (2010) Optical activation of lateral amygdala pyramidal cells instructs associative fear learning. *Proc Natl Acad Sci U S A,* 107**,** 12692-7.

Kalin, N. H., Shelton, S. E. & Davidson, R. J. (2004) The role of the central nucleus of the amygdala in mediating fear and anxiety in the primate. *J Neurosci,* 24**,** 5506-15.

Kosmal, A., Malinowska, M. & Kowalska, D. M. (1997) Thalamic and amygdaloid connections of the auditory association cortex of the superior temporal gyrus in rhesus monkey (Macaca mulatta). *Acta Neurobiol Exp (Wars),* 57**,** 165-88.

Ledoux, J. (1996) Emotional networks and motor control: a fearful view. *Prog Brain Res,* 107**,** 437-46.

Ledoux, J. (1998) Fear and the brain: where have we been, and where are we going? *Biol Psychiatry,* 44**,** 1229-38.

Lehman, M. N., Winans, S. S. & Powers, J.B. (1980) Medial nucleus of the amygdala mediates chemosensory control of male hamster sexual behavior. *Science,* 210**,** 557-60.

Mcdonald, A. J. (1998) Cortical pathways to the mammalian amygdala. *Prog Neurobiol,* 55**,** 257-332.

Mcneill, D. & Freiberger, P. (1993) *Fuzzy logic,* New York, Simon & Schuster.

Mehler, W. R. (1980) Subcortical afferent connections of the amygdala in the monkey. *J Comp Neurol,* 190**,** 733-62.

Nacewicz, B. M., Dalton, K. M., Johnstone, T., Long, M. T., Mcauliff, E. M., Oakes, T. R., Alexander, A. L. & Davidson, R. J. (2006) Amygdala volume and nonverbal social impairment in adolescent and adult males with autism. *Arch Gen Psychiatry,* 63**,** 1417-28.

Phillips, M. L., Drevets, W.C., Rauch, S.L. & Lane, R. (2003) Neurobiology of emotion perception II: Implications for major psychiatric disorders. *Biol Psychiatry,* 54**,** 515-28.

Pitkanen, A. & Amaral, D. G. (1998) Organization of the intrinsic connections of the monkey amygdaloid complex: projections originating in the lateral nucleus. *J Comp Neurol,* 398**,** 431-58.

Pitkanen, A., Savander, V. & Ledoux, J. E. (1997) Organization of intra-amygdaloid circuitries in the rat: an emerging framework for understanding functions of the amygdala. *Trends Neurosci,* 20**,** 517-23.

Price, J. L. (1981) The efferent projections of the amygdaloid complex in the rat, cat and monkey. IN BEN-ARI, Y. (Ed.) *The Amygdaloid Complex.* Amsterdam, Elsevier/North Holland Biomedical Press.

Price, J. L. (1986) Subcortical projections from the amygdaloid complex. *Adv Exp Med Biol,* 203**,** 19-33.

Price, J. L. & Amaral, D. G. (1981) An autoradiographic study of the projections of the central nucleus of the monkey amygdala. *J Neurosci,* 1**,** 1242-59.

Price, J. L., Russchen, F. T. & Amaral, D. G. (1987) The limbic region. II. The amygdaloid complex. In Björklund, A., Hökfelt, T. & Swanson, L. W. (Eds.) *Handbook of Chemical Neuroanatomy. Integrated Systems of the CNS.* Amsterdam, Elsevier Science Publishers BV.

Pujol, J., Soriano-Mas, C., Gispert, J. D., Bossa, M., Reig, S., Ortiz, H., Alonso, P., Cardoner, N., Lopez-Sola, M., Harrison, B. J., Deus, J., Menchon, J. M., Desco, M. & Olmos, S. (2010) Variations in the shape of the frontobasal brain region in obsessive-compulsive disorder. *Hum Brain Mapp*.

Rauch, S. L., Shin, L. M. & Wright, C. I. (2003) Neuroimaging studies of amygdala function in anxiety disorders. *Ann N Y Acad Sci,* 985**,** 389-410.

Reese, T. G., Heid, O., Weisskoff, R. M. & Wedeen, V. J. (2003) Reduction of eddy-current-induced distortion in diffusion MRI using a twice-refocused spin echo. *Magn Reson Med,* 49**,** 177-82.

Russchen, F. T., Bakst, I., Amaral, D. G. & Price, J. L. (1985) The amygdalostriatal projections in the monkey. An anterograde tracing study. *Brain Res,* 329**,** 241-57.

Solano-Castiella, E., Anwander, A., Lohmann, G., Weiss, M., Docherty, C., Geyer, S., Reimer, E., Friederici, A. D. & Turner, R. (2010) Diffusion tensor imaging segments the human amygdala in vivo. *Neuroimage,* 49**,** 2958-65.

Stefanacci, L. & Amaral, D. G. (2000) Topographic organization of cortical inputs to the lateral nucleus of the macaque monkey amygdala: a retrograde tracing study. *J Comp Neurol,* 421**,** 52-79.

Stefanacci, L. & Amaral, D. G. (2002) Some observations on cortical inputs to the macaque monkey amygdala: an anterograde tracing study. *J Comp Neurol,* 451**,** 301-23.

Swanson, L. W. & Petrovich, G. D. (1998) What is the amygdala? *Trends Neurosci,* 21**,** 323-31.

Turner, B. H., Mishkin, M. & Knapp, M. (1980) Organization of the amygdalopetal projections from modality-specific cortical association areas in the monkey. *J Comp Neurol,* 191**,** 515-43.

Vogt, B. A. & Pandya, D. N. (1987) Cingulate cortex of the rhesus monkey: II. Cortical afferents. *J Comp Neurol,* 262**,** 271-89.

Yukie, M. (2002) Connections between the amygdala and auditory cortical areas in the macaque monkey. *Neurosci Res,* 42**,** 219-29.

Chapter 3

Structural connectivity of the developing human amygdala[3]

The amygdala is repeatedly implicated in psychiatric & developmental disorders, but little is known about its ontogeny in humans. While there are no large developmental changes in the volume of the amygdala, functional changes do exist, as corroborated by behavioral and neuroimaging studies. Given previously reported whole-brain changes in white matter volume that occur through childhood, one possible basis for these functional differences could be the maturation of amygdalar connections with the rest of the brain. Using a recently developed tractographic method that provides a non-invasive means with which to quantify the connectivity of the amygdala as a whole and of its four main nucleus groups, we tested the hypothesis that the structural connectivity of this region changes with age. We report that amygdala connectivity is higher in children than in adults and specific to certain cortical and subcortical regions. The developmental decreases in connectivity are specific to subregions of the amygdala and their connections with cortical and subcortical brain regions related to social inference and contextual memory. These findings are informative for future research in exploring how anatomical connectivity may constrain functional maturation or dysfunction and demonstrates the use of this method in assessing structural connectivity in general.

[3] Saygin, Z.M., Osher, D.E, Koldewyn, K., Martin, R., Finn, A., Saxe, R., Gabrieli, J.D.E., Sheridan, M. (in preparation for submission).

3.1 Introduction

Amygdala Development.

The amygdala is critically involved in a variety of affective phenomena (e.g. LeDoux 1996) and has been widely implicated as the seat of dysfunction in psychiatric disorders (Engel, Bandelow et al. 2009; Damsa, Kosel et al. 2009). Many disorders with known amygdala involvement (e.g. generalized anxiety disorder, social anxiety, and autism) have their roots in development (Pine 2007; Baron-Cohen, Ring et al. 2000; Lonigan and Phillips 2001) and the amygdala appears to be important for socio-emotional development in general (Kagan and Snidman 1991). However little is known about the connectional and functional ontogeny of the amygdala in humans, especially with regard to the amygdala's different nuclei which have different functional properties. What we do know from human functional neuroimaging studies suggests that amygdala function as a whole continues to mature through adolescence (e.g. Thomas, Drevets et al. 2001; Monk, McClure et al. 2003; Killgore and Yurgelun-Todd 2006). The findings concerning structural development of the amygdala are more mixed. While several studies find that there are no developmental changes in amygdalar volume (Caviness Jr, Kennedy et al. 1996; Lebel, Walker et al. 2008), others find that there are differential effects for girls and boys (Giedd, Lalonde et al. 2009) or small increases in the volume of the amygdala relative to total brain volume (Ostby, Tamnes et al. 2009). Given the inconsistency of observations of developmental change in volume of the amygdala, and the consistent observations of developmental change in amygdala function, we hypothesize that the maturing connectivity patterns of the amygdala may be the structural change that underlies the functional development of this region.

Studies in non-human primates support this hypothesis. While neurogenesis of the amygdala is complete prenatally in non-human primates (Kordower, Piecinski et al. 1992), its projections to and from other regions mature well after birth, with connections being eliminated and refined through adulthood, in tandem with affective and social maturational milestones (Webster, Ungerleider et al. 1991a,b; Bouwmeester, Smits et al. 2002; Bouwmeester, Wolterink et al. 2002; Kalin, Shelton et al. 2001). Also, similar to observations in humans, studies in non-human primates suggest a crucial role for the amygdala in early social behavior and emotional learning. For instance, neonatal amygdala lesions in macaques lead to social deficits and/or affective problems, which may be more pronounced than lesions introduced in adulthood (Thompson, Schwartzbaum et al. 1969; Bachevalier 1994; Malkova, Mishkin et al. 2010; Bauman, Lavenex et al. 2004). Remarkably, neonatally-lesioned macaques display increased fear responses specifically to social interactions (Prather, Lavenex et al. 2001) while adult lesions produce decreased fear responses in social contexts (Emery, Capitanio et al. 2001). These studies imply that regions other than the amygdala generate fear behavior in early development. Similarly human neuroimaging studies suggest differences in amygdala function in development, and that the amygdala does not necessarily store appropriate social knowledge, but is essential for learning and relaying this information to other regions. These deficits highlight the importance of the amygdala's connectivity patterns in determining its function in the maturing brain.

White Matter Development.

The developing brain undergoes changes in white matter, most probably related to functional modifications that eventually lead to network refinement. White matter integrity has been characterized volumetrically through anatomical T1-weighted imaging, and recently, by measures using diffusion weighted imaging (DWI). Developmental changes in white matter in humans, as revealed by DWI, include increases in fractional anisotropy (FA) and decreases in mean diffusivity (MD), the average magnitude of water diffusion, indicators of white matter coherence and axonal organization (Asato, Terwilliger et al. 2010; Colby, Van Horn et al. 2011; Lebel, Walker et al. 2008). Some of the changes occur well into adulthood in tracts such as the uncinate fasciculus (Lebel, Walker et al. 2008).

Current Study.

While previous studies have focused on FA or MD, this analysis focuses on the probability of connections between the amygdala and the rest of the brain using tractography. Where FA and MD measured across the whole brain can give a sense of general white matter development, studying the amygdala's connectivity patterns across development can be informative about specific connections, which in turn can suggest hypotheses about the bases of functional maturation. In this study we use a recently developed tractographic method that provides a non-invasive means with which to describe amygdala connectivity. First we test the hypothesis that the structural

connectivity of this region changes with age. Next, by developing a model to predict an individual's age based on amygdala connectivity, we explore which brain regions' connectivity with the amygdala is most informative about these developmental changes. Finally, we utilize a probabilistic map of amygdala subregions derived from a novel method of using known connections of the subregions to segment the amygdala into four subregions. With this, we compare the maturation of the amygdala's subregions and their specific connections.

3.2 Methods

Participants.

All participants were recruited from the greater Boston area and were screened for history of mental illness. These participants fell into two groups, each containing multiple age ranges: Group 1 children (n = 28; 13 females; mean age ± standard error = 8.12 years ± 0.32), adolescents (n = 9; 3 females; mean age = 14.27 years ± 0.33), and adults (n = 27; 13 females; mean age = 23.74 years ± 0.67); and Group 2 children (n = 66; 18 females; mean age = 8.07 years ± 0.21), and adults (n = 36; 22 females; mean age = 23.44 years ± 0.56). Participants in these two groups were part of different studies using functional magnetic resonance imaging (fMRI). All participants were recruited as part of studies approved by the Massachusetts Institute of Technology, and either Children's Hospital Boston or Massachusetts General Hospital ethics committees. All participants in this study were typically developing and prior to scanning were screened for MR contraindications and known neurological abnormalities.

Acquisition.

Diffusion-weighted data were acquired from all participants using echo planar imaging (64 slices, voxel size 2x2x2mm, 128x128 base resolution, b-value 700s/mm^2, diffusion weighting isotropically distributed along 60 directions for Group 1 participants, and 30 for Group 2 participants) on a 3T Siemens scanner with a 32 channel head-

coil{Reese, 2003 #37}. A high resolution ($1mm^3$) 3D magnetization-prepared rapid acquisition with gradient echo (MPRAGE) scan was also acquired on all participants.

Tractography.

Automated cortical and subcortical parcellation was performed to define specific cortical and subcortical regions in each individual's T1 scan using FreeSurfer (Fischl, Salat et al. 2002; Fischl, van der Kouwe et al. 2004). Automated segmentation results were reviewed for quality control, and corrected for parcellation errors if necessary. They were then registered to each individual's diffusion images, and used as the seed and target regions for fiber tracking. This resulted in 85 cortical and subcortical targets and 2 seed regions (the bilateral amygdala) per participant. The principal diffusion directions were calculated per voxel, and probabilistic diffusion tractography was carried out using FSL-FDT (Behrens, Johansen-Berg et al. 2003; Behrens, Berg et al. 2007; Tomassini, Jbabdi et al. 2007) with 25000 streamline samples in each seed voxel to create a connectivity distribution to each of the target regions, while avoiding a mask consisting of the ventricles.

Tractographic analysis.

All analyses were performed on subject-specific anatomy, rather than extrapolation from a template brain. Each amygdala voxel was assigned a probability of connectivity to each target region. In each subject, the connection probability was calculated to cortical

and subcortical target regions per amygdala voxel, and normalized the distribution of probabilities for each seed voxel to [0,1], as previously reported(Saygin, Osher et al. 2011). This method of normalizing probabilities per voxel allows for a comparison of relative probabilities to each target both within and across subjects.

Amygdala volume comparisons.

The volume (in mm^3) of the right and left amygdalae were compared across age for each hemisphere using a full-factorial univariate analysis of variance for age, gender, and group (to account for any possible differences across study participants). Significance levels for main effects and interactions were determined as $P < .05$, Bonferroni corrected for the two hemispheric tests.

Connectivity differences across age.

The mean connection probability across all ipsilateral targets of the amygdala was calculated. These mean connection probabilities were modeled (separately for right and left amygdala) for effects of age, gender, and group using a full-factorial univariate model. A Pearson's partial correlation (controlling for gender and group) of mean connectivity values with age was also performed. All significance levels were set at $P < .05$, Bonferroni corrected for two hemispheric tests.

Specific connectivity changes with age.

We used a machine-learning approach (Support Vector Machine, SVM) to model the relationship between age and amygdala connectivity, since such approaches are robust to noise and are flexible even with high-dimensional data (Vapnik 2000; Ben-Hur, Ong et al. 2008) and informative for determining which features (amygdala connectivity to each ipsilateral target) of a dataset are most relevant for modeling the dependent variable (age). With an SVM, each sample is treated as a point in n-dimensional space, where n is the number of features (connectivity data); the SVR then finds the regression line that best fits the points in this hyperspace. Here, the connectivity data of ipsilateral targets to the right and left amygdalae were used as features to model chronological age with a nested leave-one-subject-out cross-validation approach (LOOCV). This was performed using in-house MATLAB (R2011b; The Mathworks, Natick, MA) code and LibSVM toolbox (http://www.csie.ntu.edu.tw/~cjlin/libsvm/).

The model was built on age and connectivity data concatenated across all but one participant, and tested using the remaining participant's connectivity data. This was performed iteratively for all participants. As is common for machine-learning approaches, we used a grid-search nested cross-validation routine in order to improve model fits while avoiding over-fitting. Within each loop of the LOOCV, optimal model parameters and features were discovered via nested cross-validation during which the remaining subjects were randomly partitioned into three groups and independently fit using ν-support vector regression with a Gaussian radial basis function kernel, varying ν (0.2, 0.5, 0.8), γ ($2^{-4:1}$), and c ($2^{-1:3}$) parameters. Features were selected by computing the Pearson correlation

coefficient separately for each nested partition, and selecting the 30 highest correlations. The model applied to the left-out subject in the outer LOOCV loop was derived from the most accurate fitting model and consensus features from the independent group of nested partitions. The relative weights of these features for predicting age from connectivity in the final model were generated by fitting a final model on all subjects using the most common parameters ($\nu = 0.8$, $\gamma = 2^{-4}$, $c = 2^{3}$), and consensus features (those features that appeared in all LOOCV loops). Since our feature selection routine was univariate, it is not influenced by issues such as multi-colinearity or redundancy, and thus reflect the features that are changing most with age. The final model weights, on the other hand, may be influenced by these factors; however, the reported correlations compliment these weights and the ordering closely follows the rank ordering of the weights.

Timing of specific connectivity changes in amygdala subregions.

We used a probabilistic atlas to explore the changes in connectivity of those same regions with specific subregions of the amygdala. The atlas was derived from a previous study (Saygin, Osher et al. 2011) that used the differential connectivity patterns of four main nuclei to segment the amygdala in adults, which and was validated through high-resolution anatomical imaging. Importantly, this method employs native-space anatomy to register amygdalae of different subjects, rather than normalization to a template, which may add unwanted warping or misalignment of data. The connectivity values for those voxels falling within the boundaries of each amygdala subregion were extracted, and ipsilateral connectivity values were averaged across right and left amygdala per individual.

Pearson's' partial correlations were performed for these connectivity values with age per nucleus, controlling for gender and study group. All significance levels were set at $P < .05$, Bonferroni corrected for the four tests of subregions.

In order to test for volumetric differences across age in the probabilistic nuclei, the number of voxels (in DWI volume) in the right and left subregions were compared across age for each hemisphere using a full-factorial univariate analysis of variance for age, gender, and group (to account for any possible differences across study participants). Significance levels for main effects and interactions were determined as $P < .05$, Bonferroni corrected for the eight tests (four tests per hemisphere). Each of the targets chosen from the model for the whole amygdala were then collapsed across hemispheres and correlated with age per nucleus using a Pearson's correlation and assessed at $P<0.05$ corrected for 13 tests per nucleus for significance. Fisher Z-tests were then used to compare correlation strengths per target for each nucleus.

3.3 Results

Connectivity differences across age.

Qualitative comparisons of probabilistic tractography maps from the bilateral amygdalae to target regions revealed higher and more widespread connection probabilities in children than in adults (**Figure 1a**). By quantifying the connectivity value of any target with the amygdala, we found that children showed higher connectivity on average than adults (**Figure 1b**) in both right (main effect of age: $F = 66.8$, $P = 9.17 \times 10^{-14}$) and left amygdalae (main effect of age: $F = 41.9$, $P = 1.16 \times 10^{-9}$).

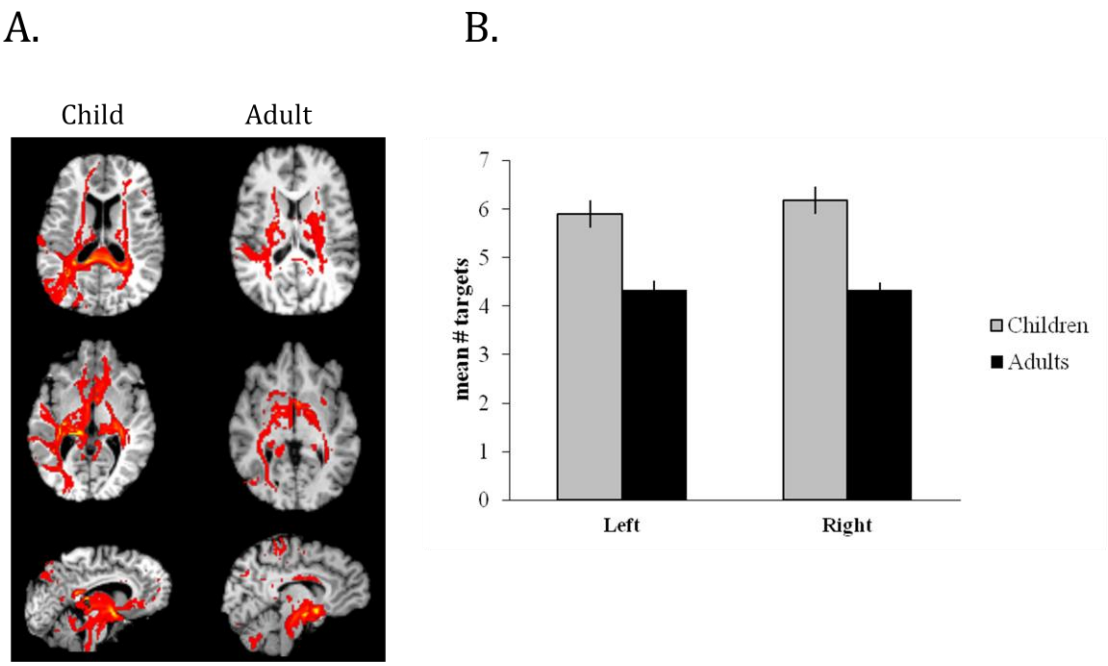

Figure 1. Overall connectivity from amygdala to target regions in children vs. adults. **A.** Probabilistic tractography maps of connectivity from the bilateral amygdalae to target regions for an example child illustrates higher and more diffuse connectivity values than the example adult participant. **B.** Children showed higher connectivity on average than adults in both right (C: $7.21 \times 10^{-2} \pm 1.55 \times 10^{-3}$, A: $5.68 \times 10^{-2} \pm 1.16 \times 10^{-3}$) and left (C: $6.87 \times 10^{-2} \pm 1.66 \times 10^{-3}$, A: $5.60 \times 10^{-2} \pm 1.49 \times 10^{-3}$).

There was no main effect of mean connectivity with gender or group (right: gender: F = 0.384, P = 0.647; group: F = 20.5, P = 0.138, left: gender: F = 0.316, P = 0.674; group: F = 10.4, P = 0.191), and no interaction of gender and/or group with age (right: gender X age: F = 1.82×10^{-2}, P = 0.893; group X age: F = 2.40, P = 0.123; gender X group X age: F = 1.39, P = 0.240, left: gender X age: F = 0.192, P = 0.662; group X age: F = 0.592, P = 0.443; gender X group X age: F = 2.06, P = 0.153).

The mean connectivity value of any target with the amygdala significantly decreased with age (**Figure 2**), again controlling for gender and group, in both the left (r = –0.452, P = 1.258×10^{-9}) and right amygdala (r = –0.531, P = 2.586×10^{-13}).

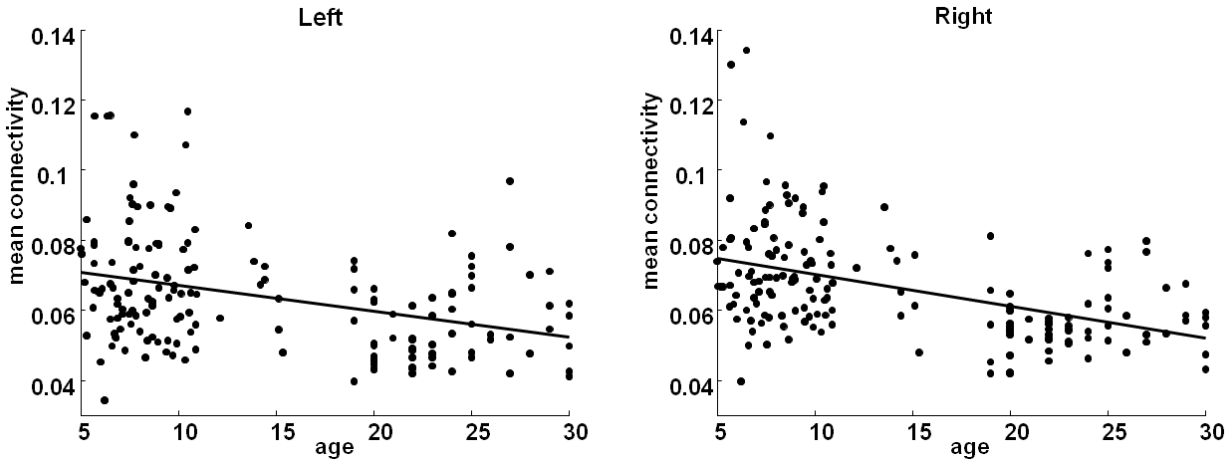

Figure 2. Mean connectivity values with age in both amygdalae. Mean connectivity values per participant are plotted by age for the left and right amygdala.

These connectivity differences across age were present despite finding no volumetric differences in the amygdala across age (main effect of age: left: $F = 2.99$, $P = 8.59 \times 10^{-2}$, right: $F = 1.07 \times 10^{-3}$, $P = 0.974$), gender, (left: $F = 3.72$, $P = 0.304$, right: $F = 0.498$, $P = 0.609$), or their interaction (genderXage: left: $F = 6.91 \times 10^{-2}$, $P = 0.793$, right: $F = 0.174$, $P = 0.677$; **Table 1**). No main effects of study group were significant (group: left: $F = 0.495$, $P = 0.610$, right: $F = 0.995$, $P = 0.501$) or interactions with age or gender were significant (group X age: left: $F = 0.422$, $P = 0.517$, right: $F = 3.03$, $P = 8.39 \times 10^{-2}$; gender X group X age: left: $F = 8.27 \times 10^{-2}$, $P = 0.774$, right: $F = 1.85$, $P = 0.175$).

Table 1. Amygdala volume in children and adults. All data are presented as mean ± s.e., in mm^3. No significant differences ($P < 0.05$ corrected for 2 tests) were found for the main effects of sex, age, or group, as well as in the interactions of sex X age and group X age in either left or right amygdala.

	Left		**Right**	
	Male	**Female**	**Male**	**Female**
Adults	1629.12 ± 34.88	1523.2 ± 27.92	1633.44 ± 32.56	1513.6 ± 27.44
Children	1572.56 ± 32.56	1453.68 ± 34.32	1656.24 ± 31.12	1525.92 ± 37.44

Specific connectivity changes with age.

In order to further understand the differences across age in connectivity patterns, we used a leave-one-out cross-validation approach to build a model that would best predict each participant's age based on the structural connectivity patterns of the amygdala. Since the model is built using only an optimal number of features (targets that the amygdala is connected with), the features that the best model ended up using would reveal the specific regions that were changing most with age. Each loop of the cross-validation model

determined at least 30 regions whose connectivity with the ipsilateral amygdala were significantly predictive of age; 26 regions were consistently chosen by the model across all cross-validation loops. Out of these consensus features, 21 of them survived Bonferroni correction for multiple comparisons ($P < 0.05/166$ cross-validation loops; **Table 2**).

Table 2. Magnitude of developmental changes. Regions used in the final SVR model, correlations with age, and the relative weights of each region in the model.

	Region	Weight	*r*	P
Decreasing with age				
Parietal	L inferior parietal	-111.77	-0.30	9.28×10^{-5}
	R inferior parietal	-107.92	-0.35	3.13×10^{-6}
	R precuneus	-104.78	-0.28	1.99×10^{-4}
	R supramarginal	-104.08	-0.31	4.00×10^{-5}
	L supramarginal	-99.22	-0.31	4.79×10^{-5}
	R superior parietal	-97.33	-0.31	5.79×10^{-5}
Occipitotemporal	R bank of STS	-107.56	-0.33	8.74×10^{-6}
	R middle temporal	-96.37	-0.34	8.56×10^{-6}
	L entorhinal	-79.58	-0.31	3.59×10^{-5}
	R entorhinal	-67.62	-0.30	9.37×10^{-5}
Basal Ganglia/Subcortical	L pallidum	-124.23	-0.39	2.41×10^{-7}
	R pallidum	-94.43	-0.40	8.26×10^{-8}
	L thalamus	-81.19	-0.309	5.02×10^{-5}
	L putamen	-70.16	-0.31	5.29×10^{-5}
	R putamen	-64.75	-0.29	1.40×10^{-4}
	L ventral diencephalon	-100.74	-0.49	1.46×10^{-11}
	R ventral diencephalon	-57.89	-0.40	1.21×10^{-7}
Increasing with age				
Medial temporal	L hippocampus	82.89	0.44	3.36×10^{-9}
	R hippocampus	103.85	0.43	6.14×10^{-9}
	L parahippocampus	133.10	0.47	1.91×10^{-10}
	R parahippocampus	146.32	0.51	2.05×10^{-12}

The optimal features that were used to model age with connectivity were specific to certain occipitotemporal, parietal, basal ganglia, and subcortical regions, many of which were bilateral (**Table 2**). Most of the regions used in the final model revealed decreasing amygdala connectivity with age, suggesting that one of the largest changes that occur in the maturing amygdala is decreasing connectivity. Each of the regions had a different contribution, or weight, to the predictions of age by connectivity. The parietal regions had some of the greatest contributions to the overall decrease in connectivity with age, followed by certain basal ganglia and other subcortical regions, including the bilateral pallidum and putamen, and occipitotemporal regions (namely middle temporal cortex and the bank of the superior temporal sulcus, or STS) which were mainly right-lateralized (**Figure 3**). The four regions with increasing connectivity, or positive weights in the model, were the bilateral hippocampus and parahippocampal cortices.

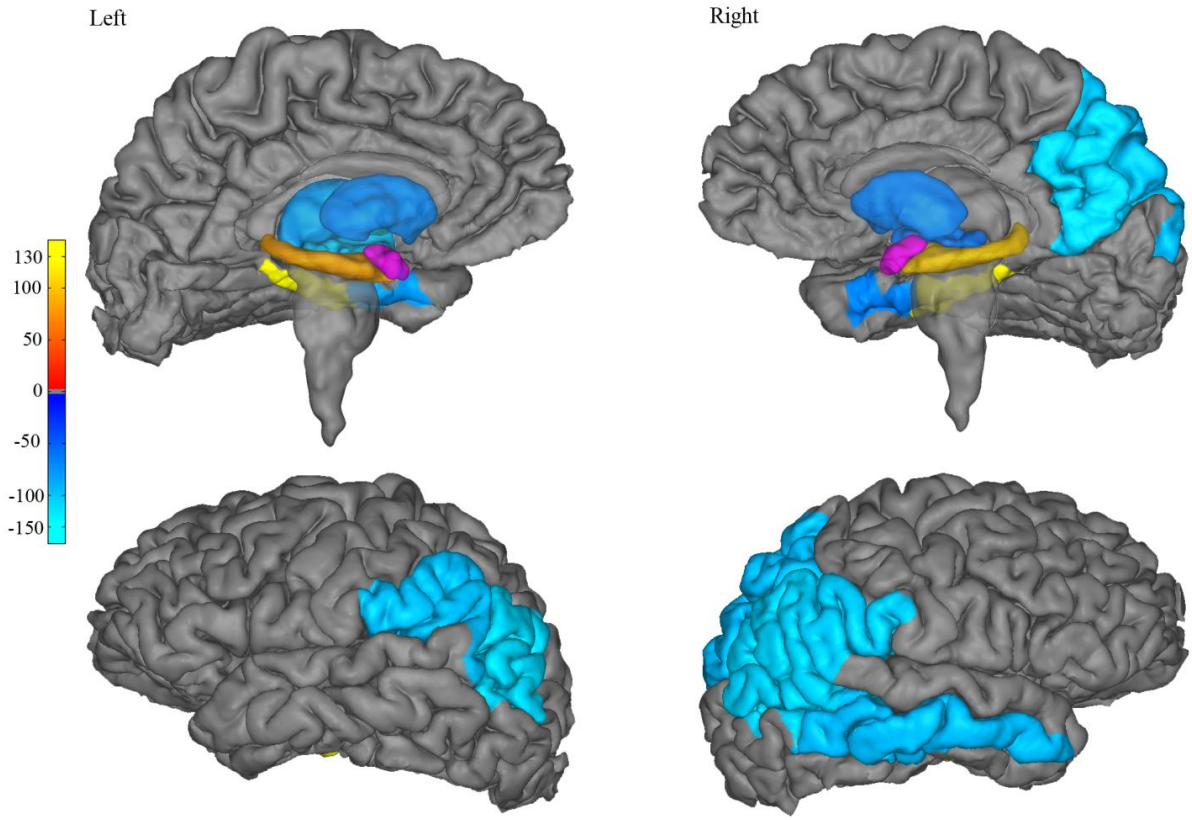

Figure 3. Connectivity changes with age. The weight, or contribution, of each target region in the final model of age by amygdala connectivity, are displayed. Negative weights represent decreasing connectivity with age, and range from dark-blue (corresponding to lower absolute weights in the model) to light-blue (higher absolute weights). Positive weights (increasing connectivity with age) are illustrated by the red- (low weights) to-yellow (high weights) colors. Right and left amygdalae are depicted in purple.

Timing of specific connectivity changes in amygdala subregions.

We next explored which subregions or nuclei of the amygdala contributed to the changes seen at the level of the whole amygdala. A probabilistic atlas of amygdala subregions, originally derived from a novel method of tractographic segmentation (Saygin, Osher et al. 2011), was overlaid on each participant's native diffusion-space amygdala. While unlikely that the probabilistic overlays would show differences in volume across age, the volume of these subregions was calculated per individual and assessed for age, gender, and study group differences. No volumetric differences in the probabilistic nuclei were found for the main effect of age, gender, group, and their interactions with age (**Table 3**).

Table 3. Volumetric measurements in the probabilistic nuclei and tests for main effects and interactions of gender, age, and study group.

		Left		**Right**	
		F	P	F	P
Gender	Basal	.525	.470	.398	.529
	Lateral	.966	.327	.454	.501
	Central	.573	.450	.077	.781
	Medial	.693	.406	.361	.549
Group	Basal	3.310	.071	.454	.501
	Lateral	.510	.476	.433	.511
	Central	.069	.793	.178	.674
	Medial	.557	.456	.314	.576
Age	Basal	2.492	.116	.059	.808
	Lateral	.037	.847	.049	.826
	Central	1.664	.199	.088	.768
	Medial	.552	.459	.078	.781
Gender* Age	Basal	.110	.741	1.167	.282
	Lateral	.712	.400	1.197	.276
	Central	.047	.828	.939	.334
	Medial	1.132	.289	1.196	.276
Group*Age	Basal	.210	.647	.218	.641
	Lateral	.078	.780	.230	.632
	Central	.561	.455	.352	.554
	Medial	.371	.543	.260	.611

Given the lack of volumetric differences across age, the developmental changes of connectivity for these subregions were explored. Since connectivity values to each target region were calculated per voxel of the amygdala, the mean connectivity values for ipsilateral targets from voxels within each probabilistic nucleus were extracted and collapsed across hemisphere. These were then correlated with age while controlling for gender and study group (**Figure 4**). The basal and lateral amygdala had a clear relationship with age (basal: $r = -0.357$, $P = 2.777 \times 10^{-6}$; lateral: $r = -0.546$, $P = 3.83 \times 10^{-14}$), as did the central to lesser extent ($r = -0.318$, $p = 3.417 \times 10^{-5}$), while the medial amygdala had mean connectivity values which were relatively stable across ages 5-30 ($r = -7.31 \times 10^{-3}$, $p = 0.093$).

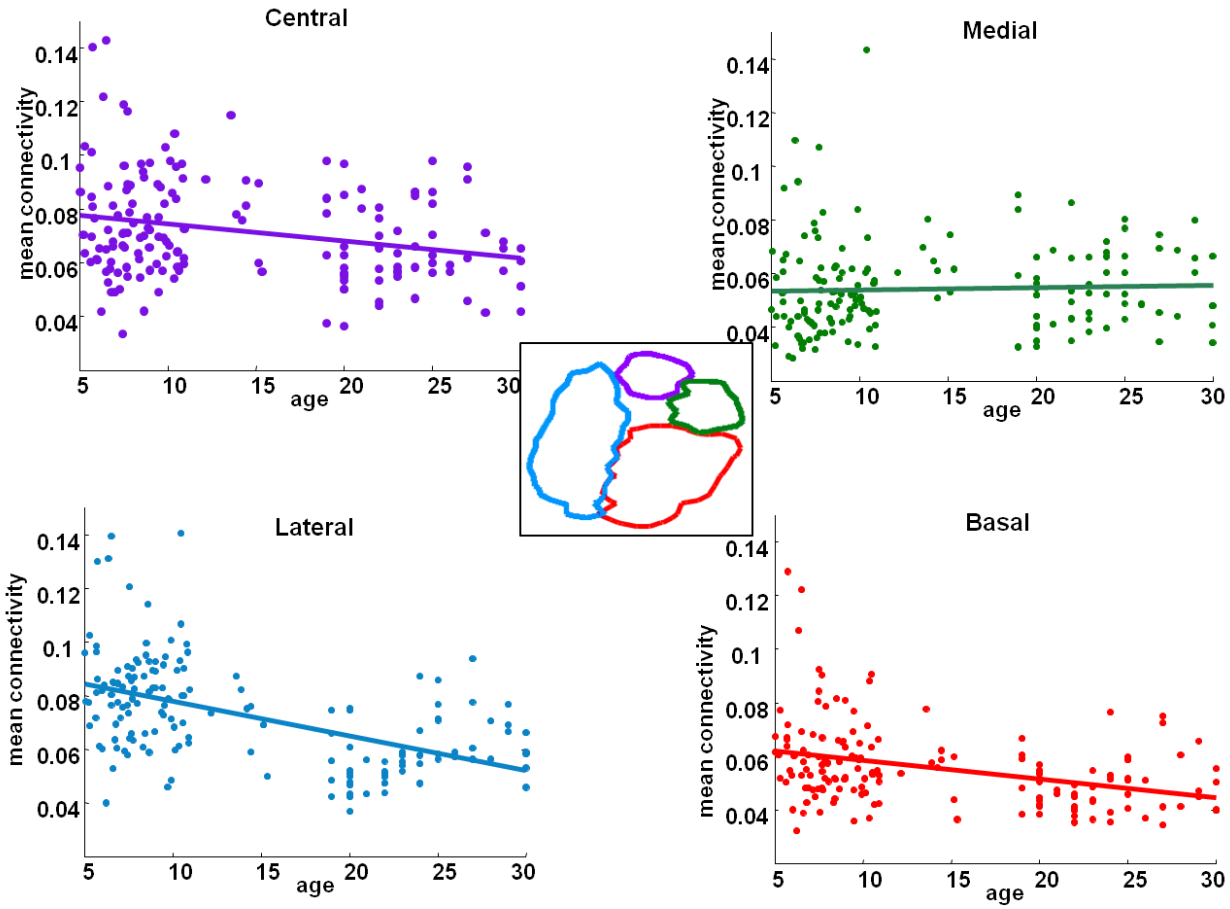

Figure 4. Correlations of age with mean connectivity for the four amygdala subregions. A probabilistic atlas of four amygdala subregions (illustrated in the center) was used to extract mean connectivity values from each subregion bilaterally per subject and plotted by age. While connectivity with the basal, lateral, and central subregions were significantly correlated with age, connectivity with the medial amygdala showed no significant change with age.

We next tested for any differences between the amygdala subregions in their connectivity changes with age for each of the individual target regions. Since the medial nucleus' connectivity patterns were not changing with age, we focused our analyses on the basal, lateral, and central nuclei. Each subregion's mean connectivity to the consensus features above (collapsed across hemisphere) were correlated with age (**Table 4**). The lateral subregion's connectivity with all of the targets except the bank of STS changed significantly with age (Bonferroni corrected at $P < 0.05/13$ regions). All but three of the basal subregion's targets (entorhinal, precuneus, and superior parietal) had significant changes with age ($P < 0.05/13$). Only 8 of the central amygdala's targets showed a significant correlation with age.

Table 4. Correlation of connectivity to target regions with age per nucleus.

	Basal		**Lateral**		**Central**	
	R	P	R	P	R	P
Inferior Parietal	-0.32	3.47×10^{-5}	-0.38	4.84×10^{-7}	-0.33	1.48×10^{-5}
Precuneus	-0.18	1.87×10^{-2}	-0.37	1.22×10^{-6}	-0.27	4.50×10^{-4}
Supramarginal	-0.27	3.69×10^{-4}	-0.36	1.90×10^{-6}	-0.32	3.40×10^{-5}
Superior Parietal	-0.19	1.37×10^{-2}	-0.34	8.34×10^{-6}	-0.28	3.28×10^{-4}
Bank of STS	-0.23	3.55×10^{-3}	-0.21	7.05×10^{-3}	-0.29	1.32×10^{-4}
Middle Temporal	-0.33	1.31×10^{-5}	-0.23	2.75×10^{-3}	-0.28	2.37×10^{-4}
Entorhinal	-0.02	0.792	-0.36	1.39×10^{-6}	-0.45	1.07×10^{-9}
Pallidum	-0.37	8.44×10^{-7}	-0.53	2.10×10^{-13}	-0.12	0.118
Putamen	-0.32	3.34×10^{-5}	-0.37	7.10×10^{-7}	-0.15	4.89×10^{-2}
Thalamus	-0.30	8.06×10^{-5}	-0.38	4.37×10^{-7}	-0.01	0.925
Ventral Diencephalon	-0.49	4.17×10^{-11}	-0.58	2.17×10^{-16}	0.04	0.576
Hippocampus	0.46	8.97×10^{-10}	0.48	3.89×10^{-11}	0.10	0.183
Parahippocampus	0.48	1.09×10^{-10}	0.48	4.15×10^{-11}	0.43	8.23×10^{-9}

To further compare amygdala subregions, we employed a Fisher's Z test for correlation coefficients of connectivity by age per target region. The basal vs. the lateral nucleus were only different in correlation strength for connectivity with entorhinal cortex ($P = 1.11x10^{-3}$), whereas both the basal nucleus and the lateral nuclei were changing with age significantly more so than the central nucleus for connectivity with the hippocampus (BvC: $P = 4.72x10^{-4}$; LvC: $P = 1.29x10^{-4}$), pallidum (BvC: $P = 1.47x10^{-2}$; LvC: $P = 2.41x10^{-5}$), thalamus (BvC: $P = 5.83x10^{-3}$; LvC: $P = 3.89x10^{-4}$), and ventral DC (BvC: $P = 2.13x10^{-7}$; LvC: $P = 1.62x10^{-10}$). Further, the lateral subregion was decreasing with age significantly more so than the central amygdala for the putamen ($P = 3.14x10^{-2}$). In sum, the central nucleus' connectivity changes with age were attributable to fewer targets than the basal and lateral, whereas the basal and lateral nuclei carried most of the changes with age seen at the level of the whole amygdala, and were quite similar to one another in correlation strengths of connectivity with age. Further, the basal and lateral subregions had significantly stronger increases in connectivity with age for hippocampal targets as compared to the central and stronger decreases in connectivity with age for basal ganglia targets while again the central nucleus remained static.

3.4 Discussion

The present results reveal that amygdala connectivity is more diffuse in children than in adults, and is on average decreasing with age in both the right and left amygdala. The connectivity patterns of each of the target regions for amygdala tractography were then modeled to predict biological age. This revealed which brain regions were driving the developmental change and to what extent they were doing so. Most of these regions decreased in their connectivity values with age, consistent with observations of pruning in development (e.g. Webster, Ungerleider et al. 1991a,b; O'Leary 1992; Luo and O'Leary 2005; Gogtay, Giedd et al. 2004).

Among the decreasing regions were the occipitotemporal cortices, as well as certain dorsal and ventral parietal regions, which altogether, carried much of the contribution to the model of amygdala connectivity with age. Many of these regions are believed to be involved in social processing and may, together with the amygdala, form a network commonly implicated in social cognition (e.g. Adolphs 2003). The decrease in connectivity with age, along with increasing specialization in functional regions such as the temporoparietal junction, or TPJ (Saxe and Kanwisher 2003), may suggest that connectivity starts out diffuse but becomes increasingly more specific as the functional roles of the target regions are better defined. This interpretation is consistent with developmental nonhuman primate studies. For instance, in infant macaques, the normal refinement of amygdala connections to brain regions that process high-level visual categories (inferior temporal cortex, TE) such as faces, emerge around the same time that social play begins; moreover, this coincides with fear and defensive responses to strangers (Kalin, Shelton et

al. 1991). In fact, in addition to adult-like projections between TE and the amygdala, projections from lower-visual area TEO to the amygdala exist in infant monkeys; in other words, amygdala-temporal projections are eliminated and refined by adulthood (Webster, Ungerleider et al. 1991a,b). Lesions of TE in infants results in the preservation of these connections between TEO and the amygdala, suggesting that before higher-order cortices fully mature, additional connections may exist as a compensatory mechanism. Evidence from studies of amygdala lesions in infant vs. adult macaques (Prather, Lavenex et al. 2001; Emery, Capitanio et al. 2001) also suggests that the amygdala is necessary for learning and relaying appropriate social information to other cortices, and that this functional role may change with normal development.

Our results of decreasing connectivity with age also provide evidence for an instructional role of the amygdala's connectivity with regions related to social processing. Future studies in humans should analyze the functional maturation of occipitotemporal and temporoparietal cortices, and directly compare them to the structural connectivity measurements of amygdala maturity as described here. It would be interesting, for instance, to assess the spatial distribution of connectivity within these regions to the amygdala (with these regions as seeds rather than targets), directly relate this to function in the region (e.g. Saygin, Osher et al. 2012) and test how this changes with age. One would hypothesize, based on the present paper, that the spatial map of connectivity to the amygdala from these cortices, would be increasingly focalized, and overlap well with specific functional regions such as the fusiform face area (Kanwisher, McDermott et al. 1997; Tsao, Freiwald et al. 2006) or the TPJ (Saxe and Kanwisher 2003). This will provide insight into the functional importance of these connectivity changes in normal

development, and help formalize more informed hypotheses about which specific regions or connections are impaired by limited or pathological social interactions during human development.

The only regions increasing in their connectivity to the amygdala with age were the parahippocampal and hippocampal regions. Given the functional role of these regions in contextual processing (Bar 2004, Eichenbaum and Lipton 2008), these findings may imply an increasing role of the amygdala for integrating emotional content for contextual processing. This type of processing in an adult organism would already involve largely noisy input which may be impractical or too complicated for an immature system to adequately parse. Contextual processing involves specific combinations of a large variety of stimuli and thus might be expected to require a large throughput and vast integration of multiple inputs as opposed to select and specific information for functional specificity, which decreasing connectivity may substrate. A natural extension of this study would be to compare the spatial distribution of amygdala connectivity across age within these regions to the parietal and occipitotemporal regions (as above) which are decreasing in connectivity, and directly relate these changes to individual function.

The analyses in the present paper further revealed that these changes in connectivity with age are specific to certain subnuclei, which is not surprising since these subnuclei have different functions (e.g. LeDoux 1998; Gloor 1997). Also, previous studies in nonhuman primates have reported that the maturation of amygdalar connections is not attributable to the connectivity of the whole structure but rather to the nucleus groups (e.g. (Webster, Ungerleider et al. 1991a,b; Rodman 1994). The analyses of the amygdala

subregions in the present paper provided evidence for this in humans and revealed that while medial nucleus connectivity remained constant with age and central nucleus connectivity exhibited little change with age, the basal and lateral nuclei best reflected the changes seen at the level of the whole amygdala, suggesting that the development of the whole amygdala is actually development at the level of these nuclei. This is perhaps to be expected, given that the lateral and basal nuclei are responsible for emotional and social learning and integrate visual stimuli with value (Freese and Amaral 2009; Baxter and Murray 2002), while the central and medial nuclei are primarily involved in motor responses to conditioned stimuli and in olfactory/gustatory responses respectively (LeDoux 1996; Lehman, Winans et al. 1980; Kalin, Shelton et al. 2004; Bian, Yanagawa et al. 2008).

The differences between the nuclei were further supported by the comparisons of nucleic connectivity to each target region and their changes with age. For cortical regions, namely the parietal and occipitotemporal cortices, connectivity patterns with the basal, lateral, and central nuclei were similar in their changes with age. However, there existed a dissociation between these nuclei's patterns of connectivity to the hippocampus and basal ganglia. These target structures are quite dissociable in function and are believed to mediate declarative (explicit) and non-declarative (implicit) learning and memory respectively; further, there is prior evidence of an antagonistic relationship between these memory systems, such that basal ganglia function can interfere with explicit or contextual memory, and hippocampal function with stimulus-response or other types of implicit learning(Packard and Knowlton 2002; Yin and Knowlton 2006). We found that this dissociable relationship was mirrored at the level of nucleus connectivity with these

regions. The central nucleus was not changing with age, while the basal and lateral which are considered to be similar to cortex due to the heavy presence of pyramidal cells, were decreasing in their connectivity and integration with the basal ganglia, and in the meantime, increasing in their connectivity with the competing memory system. This suggests that the central amygdala is already mature in its connections with these memory systems at age five, the earliest age group for this study, while the basal and especially the lateral nucleus, are undergoing opposing developmental changes in its connectivity with these competitively interacting memory systems.

In summary, we have shown that amygdala connectivity to cortical and subcortical regions changes with age. Connectivity with cortical targets was observed to primarily decrease with age and was specific to regions related to social learning and visual integration, suggesting a structural substrate for the amygdala's development for such functions. Connectivity with subcortical regions was also changing with age, and was specific to the basal and lateral nuclei of the amygdala. The hippocampus and basal ganglia, known to mediate explicit vs. implicit learning, were found to have competing developmental changes in connectivity with these nuclei (increasing vs. decreasing, respectively). The different types of changes in structural connectivity that were reported here would be useful for sculpting the precise connectivity patterns seen in adulthood and are perhaps related to the different functions of the amygdala, such as integrating emotional content into contextual processing or learning appropriate social nuances. Future studies can further explore such hypotheses about how structural maturation can subserve function.

3.5 References

Adolphs, R. (2003). "Cognitive neuroscience of human social behaviour." Nature Reviews Neuroscience **4**(3): 165-178.

Asato, M., R. Terwilliger, et al. (2010). "White matter development in adolescence: a DTI study." Cerebral Cortex **20**(9): 2122-2131.

Bachevalier, J. (1994). "Medial temporal lobe structures and autism: a review of clinical and experimental findings." Neuropsychologia **32**(6): 627-648.

Bar, M. (2004). "Visual objects in context." Nature Reviews Neuroscience **5**(8): 617-629.

Baron-Cohen, S., H. A. Ring, et al. (2000). "The amygdala theory of autism." Neurosci Biobehav Rev **24**(3): 355-64.

Bauman, M., P. Lavenex, et al. (2004). "The development of mother-infant interactions after neonatal amygdala lesions in rhesus monkeys." The Journal of neuroscience **24**(3): 711-721.

Baxter, M. and E. Murray (2002). "The amygdala and reward." NATURE REVIEWS NEUROSCIENCE **3**(7): 563-573.

Behrens, T. E., H. J. Berg, et al. (2007). "Probabilistic diffusion tractography with multiple fibre orientations: What can we gain?" Neuroimage **34**(1): 144-55.

Behrens, T. E., H. Johansen-Berg, et al. (2003). "Non-invasive mapping of connections between human thalamus and cortex using diffusion imaging." Nat Neurosci **6**(7): 750-7.

Ben-Hur, A., C. S. Ong, et al. (2008). "Support vector machines and kernels for computational biology." PLoS computational biology **4**(10): e1000173.

Bian, X., Y. Yanagawa, et al. (2008). "Cortical-like functional organization of the pheromone-processing circuits in the medial amygdala." J Neurophysiol **99**(1): 77-86.

Bouwmeester, H., K. Smits, et al. (2002). "Neonatal development of projections to the basolateral amygdala from prefrontal and thalamic structures in rat." The Journal of comparative neurology **450**(3): 241-255.

Bouwmeester, H., G. Wolterink, et al. (2002). "Neonatal development of projections from the basolateral amygdala to prefrontal, striatal, and thalamic structures in the rat." The Journal of comparative neurology **442**(3): 239-249.

Caviness Jr, V., D. Kennedy, et al. (1996). "The human brain age 7â€“11 years: a volumetric analysis based on magnetic resonance images." Cerebral Cortex **6**(5): 726-736.

Colby, J. B., J. D. Van Horn, et al. 2011 ("Quantitative in vivo evidence for broad regional gradients in the timing of white matter maturation during adolescence." Neuroimage **54**(1): 25-31.

Damsa, C., M. Kosel, et al. (2009). "Current status of brain imaging in anxiety disorders." Current opinion in psychiatry **22**(1): 96.

Eichenbaum, H. and P. A. Lipton (2008). "Towards a functional organization of the medial temporal lobe memory system: role of the parahippocampal and medial entorhinal cortical areas." Hippocampus **18**(12): 1314-1324.

Emery, N., J. Capitanio, et al. (2001). "The effects of bilateral lesions of the amygdala on dyadic social interactions in rhesus monkeys (Macaca mulatta)." Behav Neurosci **115**(3): 515-44.

Engel, K., B. Bandelow, et al. (2009). "Neuroimaging in anxiety disorders." Journal of Neural Transmission **116**(6): 703-716.

Fischl, B., D. H. Salat, et al. (2002). "Whole brain segmentation: automated labeling of neuroanatomical structures in the human brain." Neuron **33**(3): 341-55.

Fischl, B., A. van der Kouwe, et al. (2004). "Automatically parcellating the human cerebral cortex." Cereb Cortex **14**(1): 11-22.

Freese, J. L. and D. G. Amaral (2009). Neuroanatomy of the Primate Amygdala. The Human Amygdala. P. J. Whalen and E. A. Phelps. New York, The Guilford Press**:** 3-42.

Giedd, J. N., F. M. Lalonde, et al. (2009). "Anatomical brain magnetic resonance imaging of typically developing children and adolescents." Journal of the American Academy of Child and Adolescent Psychiatry **48**(5): 465.

Gloor, P. (1997). The Temporal Lobe and Limbic System. New York, New York, Oxford University Press, Inc.

Gogtay, N., J. N. Giedd, et al. (2004). "Dynamic mapping of human cortical development during childhood through early adulthood." Proceedings of the National Academy of Sciences of the United States of America **101**(21): 8174.

Kagan, J. and N. Snidman (1991). "Temperamental factors in human development." American Psychologist **46**(8): 856.

Kalin, N. H., S. E. Shelton, et al. (2004). "The role of the central nucleus of the amygdala in mediating fear and anxiety in the primate." J Neurosci **24**(24): 5506-15.

Kalin, N. H., S. E. Shelton, et al. (2001). "The primate amygdala mediates acute fear but not the behavioral and physiological components of anxious temperament." The Journal of neuroscience **21**(6): 2067-2074.

Kalin, N. H., S. E. Shelton, et al. (1991). "Defensive behaviors in infant rhesus monkeys: ontogeny and contextâ€dependent selective expression." Child development **62**(5): 1175-1183.

Kanwisher, N., J. McDermott, et al. (1997). "The fusiform face area: a module in human extrastriate cortex specialized for face perception." J Neurosci **17**(11): 4302-11.

Killgore, W. and D. Yurgelun-Todd (2006). "Ventromedial prefrontal activity correlates with depressed mood in adolescent children." Neuroreport **17**(2): 167-71.

Kordower, J. H., P. Piecinski, et al. (1992). "Neurogenesis of the amygdaloid nuclear complex in the rhesus monkey." Developmental brain research **68**(1): 9-15.

Lebel, C., L. Walker, et al. (2008). "Microstructural maturation of the human brain from childhood to adulthood." Neuroimage **40**(3): 1044-1055.

LeDoux, J. (1996). "Emotional networks and motor control: a fearful view." Prog Brain Res **107**: 437-46.

LeDoux, J. (1998). "Fear and the brain: where have we been, and where are we going?" Biol Psychiatry **44**(12): 1229-38.

Lehman, M. N., S. S. Winans, et al. (1980). "Medial nucleus of the amygdala mediates chemosensory control of male hamster sexual behavior." Science **210**(4469): 557-60.

Lonigan, C. J. and B. M. Phillips (2001). "Temperamental influences on the development of anxiety disorders."

Luo, L. and D. D. M. O'Leary (2005). "Axon retraction and degeneration in development and disease." Annu. Rev. Neurosci. **28**: 127-156.

Malkova, L., M. Mishkin, et al. (2010). "Long-term effects of neonatal medial temporal ablations on socioemotional behavior in monkeys (Macaca mulatta)." Behavioral neuroscience **124**(6): 742.

Monk, C. S., E. B. McClure, et al. (2003). "Adolescent immaturity in attention-related brain engagement to emotional facial expressions." Neuroimage **20**(1): 420-428.

O'Leary, D. D. M. (1992). "Development of connectional diversity and specificity in the mammalian brain by the pruning of collateral projections." Current Opinion in Neurobiology **2**(1): 70-77.

Ostby, Y., C. K. Tamnes, et al. (2009). "Heterogeneity in subcortical brain development: a structural magnetic resonance imaging study of brain maturation from 8 to 30 years." The Journal of neuroscience **29**(38): 11772-11782.

Packard, M. G. and B. J. Knowlton (2002). "Learning and memory functions of the basal ganglia." Annual review of neuroscience **25**(1): 563-593.

Pine, D. S. (2007). "Research review: a neuroscience framework for pediatric anxiety disorders." Journal of Child Psychology and Psychiatry **48**(7): 631-648.

Prather, M., P. Lavenex, et al. (2001). "Increased social fear and decreased fear of objects in monkeys with neonatal amygdala lesions." Neuroscience **106**(4): 653-658.

Rodman, H. R. (1994). "Development of inferior temporal cortex in the monkey." Cerebral Cortex **4**(5): 484-498.

Saxe, R. and N. Kanwisher (2003). "People thinking about thinking people:: The role of the temporo-parietal junction in." Neuroimage **19**(4): 1835-1842.

Saygin, Z. M., D. E. Osher, et al. (2011). "Connectivity-based segmentation of human amygdala nuclei using probabilistic tractography." Neuroimage **56**(3): 1353-1361.

Saygin, Z. M., D. E. Osher, et al. (2012). "Anatomical connectivity patterns predict face selectivity in the fusiform gyrus." Nature Neuroscience **15**, 321-327.

Thomas, K., W. Drevets, et al. (2001). "Amygdala response to facial expressions in children and adults." BIOLOGICAL PSYCHIATRY **49**(4): 309-316.

Thompson, C., J. Schwartzbaum, et al. (1969). "Development of social fear after amygdalectomy in infant rhesus monkeys." Physiology & Behavior **4**(2): 249-254.

Tomassini, V., S. Jbabdi, et al. (2007). "Diffusion-weighted imaging tractography-based parcellation of the human lateral premotor cortex identifies dorsal and ventral subregions with anatomical and functional specializations." The Journal of neuroscience **27**(38): 10259-10269.

Tsao, D. Y., W. A. Freiwald, et al. (2006). "A cortical region consisting entirely of face-selective cells." Science **311**(5761): 670-4.

Vapnik, V. N. (2000). The nature of statistical learning theory, Springer-Verlag New York Inc.

Webster, M., L. Ungerleider, et al. (1991a). "Connections of inferior temporal areas TE and TEO with medial temporal-lobe structures in infant and adult monkeys." The Journal of neuroscience **11**(4): 1095-1116.

Webster, M. J., L. G. Ungerleider, et al. (1991b). "Lesions of inferior temporal area TE in infant monkeys alter cortico-amygdalar projections." Neuroreport: An International Journal for the Rapid Communication of Research in Neuroscience.

Yin, H. H. and B. J. Knowlton (2006). "The role of the basal ganglia in habit formation." Nature Reviews Neuroscience **7**(6): 464-476.

Chapter 4

Tracking early reading development: White matter volume and integrity correlate with phonological awareness in children before formal reading instruction[4]

Developmental dyslexia, an unexplained difficulty in learning to read, has been associated in children and adults with alterations in white matter organization as measured by diffusion-weighted imaging (DWI). It is unknown, however, whether these differences in structural connectivity are related to the cause of dyslexia, or instead are consequences of reading difficulty (e.g., less reading experience or compensatory brain organization). Here, in 20 kindergartners who had received little or no reading instruction, we examined the relation between major behavioral predictors of dyslexia, including phonological awareness (PA) for language sounds, and white-matter organization in three tracts (inferior longitudinal, ILF; arcuate fasciculus, SLFa; parietal sect ion of superior longitudinal fasciculus, SLFp) using probabilistic tractography. Superior composite PA scores were significantly and positively correlated with volume and axial diffusivity (AD) of the left SLFa, but not with any other tract measures, including control measures. Other behavioral predictors of dyslexia did not correlate with DWI values in these tracts. The volume, AD, and fractional anisotropy (FA) of left SLFa was positively correlated with the phoneme blending subtest specifically, and not with other PA tasks. These findings reveal that the left SLFa, which has been frequently associated with poor reading in previous studies, is already smaller and has lower FA and AD in kindergarteners at risk for dyslexia because of poor PA. These findings suggest a structural basis of risk for dyslexia that predates reading instruction.

[4] Saygin Z.M.*, Norton E.S.*, Osher D.E., Beach S. B., Cyr A.B., Ozranov-Palchik O., Yendiki A., Fischl B., Gaab N., Gabrieli J.D.E. (in submission to J.Neurosci. 2012)

4.1 Introduction

Developmental dyslexia, an unexplained difficulty in learning to read, affects approximately 10% of children in the US and is associated with atypical brain function for reading, especially reduced activations in left temporo-parietal regions (Lyon et al., 2003; Gabrieli, 2009) that are independent of current reading ability (Hoeft et al., 2007) or estimated IQ (Tanaka et al., 2011). Dyslexia has also been associated with structural differences in white matter organization as measured by diffusion weighted imaging (DWI), specifically lower fractional anisotropy (FA) in the left hemisphere (Klingberg et al., 2000; Rimrodt et al., 2010; Steinbrink et al., 2008). These differences may reflect weakened white-matter connectivity among the core constituents of a left-hemisphere network that supports fluent reading. This interpretation is bolstered by evidence that similar DWI measures correlate with reading skill even among typical readers (Klingberg et al. 2000; Deutsch et al., 2005).

A fundamental question is whether these white-matter structural differences are a cause or a consequence of poor reading in dyslexia. Prior DWI studies have not yet answered this question because they have involved children and adults with years of reading experience, and children with reading difficulty read far less than typically reading children (Cunningham et al. 1998) and appear to develop alternative reading strategies (e.g., dyslexic children often exhibit enhanced right-hemisphere activation; Shaywitz et al. 2002). The most direct way to evaluate whether white-matter differences may contribute to the etiology of dyslexia is to examine such differences in pre-reading children (i.e.

kindergartners) in whom reading instruction and experience is unlikely to influence brain structure.

Pre-reading children cannot exhibit dyslexia per se, but they can be evaluated for reading-related skills that are impaired in dyslexia and that predict dyslexia in pre-readers. The three best predictors of future reading ability in English are Phonological Awareness (awareness of the sound structure of spoken words, which must be mapped onto letters to learn to read), Rapid Automatized Naming, and Letter Knowledge (Schatschneider et al., 2004). Some studies in reading individuals have reported relations between white-matter structure and phonological awareness. Children ages 7-11 with superior Phonological Awareness had stronger white-matter organization in callosal fibers connecting the temporal lobes (Dougherty et al., 2007). In adults, Phonological Awareness correlated positively with the volume of the left superior longitudinal fasciculus (Frye et al., 2011) and with higher FA of the left arcuate fasciculus (Vandermosten et al., 2012). The left arcuate fasciculus is part of the superior longitudinal fasciculus and connects temporoparietal and inferior frontal regions that are the core constituents of the language network.

We hypothesized that if white-matter differences are related to the cause of dyslexia, then such differences ought to be related to the skills in pre-readers that are known to predict future reading ability. We therefore behaviorally characterized kindergartners (mostly 5 year-olds) and performed DWI in those children. We examined several tracts, with a particular focus on the left arcuate fasciculus because of its importance in language, and because of its association with Phonological Awareness in older readers.

4.2 Methods

Overview

As part of a larger study, kindergarten children completed a short battery of psycho-educational screening assessments in their schools in eastern Massachusetts within the first eight weeks of the school year, before reading instruction. A subset of these children with varying pre-reading skills was invited to take part in brain imaging. This study was approved by IRBs at MIT and Children's Hospital Boston. Parents gave written consent and children gave verbal assent to participate.

Participants

DWI data were collected from 24 children. Of these, 4 children had excessive motion and were excluded from subsequent analysis. Analyses included 20 children (demographic information and scores in **Table 1**). All children met eligibility criteria, which included: native speaker of American English; born at 36 weeks gestation or more; no sensory or perceptual difficulties other than corrected vision; no history of head or brain injury or trauma; no neurological/neuropsychological/developmental diagnoses; no medications affecting the nervous system; standard scores greater than 80 on measures of nonverbal and verbal IQ (Kaufman Brief Intelligence Test-2 Matrices; Peabody Picture Vocabulary Test-IV).

Table 1. Demographic information and scores for participants (n=20).

Measure	Mean	SD	Range
Age (months)	66.9	4.7	60-76
KBIT-2 Matrices SS	102.4	11.1	85-120
PPVT-IV SS	116.4	16.5	83-160
LK Composite SS	107.7	10.4	89-132
RAN Composite SS	96.2	13.5	68-117
PA Composite SS	10.3	2.2	7-15
BSMSS	51.6	10.6	29.5-66

KBIT=Kaufman Brief Intelligence Test; PPVT=Peabody Picture Vocabulary Test. PA=Phonological Awareness; RAN=Rapid Automatized Naming; LK=Letter Knowledge SS=Standard Score, where standardized mean is 100, except for PA, which is 10. BSMSS=Barratt Simplified Measure of Social Status, possible range: 8-66.

Behavioral Measures

Phonological awareness.

Three subtests from the Comprehensive Test of Phonological Processing (CTOPP; Wagner et al., 1999) were given to assess awareness of and ability to manipulate phonological structures. Subtests given were: 1) Elision: the child repeats a word after removing a given sound (e.g. "say boat without saying /b/"); 2) Blending Words: the child listens to a recorded word produced sound-by-sound and puts the sounds together to derive a real word; 3) Nonword Repetition: the child listens to a recording of a made-up word (like "sart") and repeats it. Raw scores for all subtests were determined from the total number of items answered correctly. A composite was created from the mean standard score for each subtest.

Letter knowledge.

The Letter Sound Knowledge subtest from the York Assessment of Reading for Comprehension (YARC; Snowling et al., 2010) was given to assess knowledge of letter sounds and phoneme isolation skills. The child is asked to give the sound that a printed letter or pair of letters (digraph) makes. The Letter Identification subtest from the Woodcock Reading Mastery Test, Revised/Normative Update (WRMT-R/NU; Woodcock, 1998) was given to assess letter name knowledge. For this test, the child is asked to give the names of printed single letters. For both tests, raw scores are determined from the total number of items answered correctly. A composite was created from the mean standard scores for the YARC and WRMT-R subtests.

Rapid automatized naming.

The RAN-RAS Tests (Wolf & Denckla, 2005) were given to measure the speed and efficiency of processes by which a series of randomly arranged stimuli are named. Subtests given were Object, Color, and Letter Naming. In each subtest, the child names a series of familiar items. Each test has 5 tokens that are repeated randomly 10 times. Raw scores are determined from the completion times for each subtest in seconds. A composite was created from the mean standard scores for each subtest. For children who could not reliably name letters, a composite was created from the Objects and Colors subtests.

Image acquisition and processing

Data were acquired on a 3T Siemens Trio Tim scanner with a standard Siemens 32-channel phased array head coil. A whole-head, high-resolution T1-weighted multi-echo MPRAGE (van der Kouwe et al. 2008; Mugler et al. 2000) anatomical volume was acquired (acquisition parameters: TR = 2350ms, TE = 1.64ms, TI = 1400ms, flip angle = 7°, FOV = 192 × 192, 176 slices, voxel resolution = 1.0mm^3, acceleration = 4 averages). An online prospective motion correction algorithm (ICE) was implemented to reduce the effect of motion artifacts during the structural scan, and 10 selective reacquisition TRs were included to replace TRs that included head motion (Tisdall et al., in press). A diffusion-weighted scan was collected using echo planar imaging with 30 independent diffusion gradient directions (b = 0 and 700s/mm^2, 128x128 base resolution, voxel resolution = 2.0mm^3).

Structural MRI data were processed using the semi-automated processing stream, using the default parameters in FreeSurfer v5.0.0 (Dale et al., 1999; Fischl et al. 2002, 2004; Desikan et al. 2009; http://surfer.nmr.mgh.harvard.edu/), which includes motion and intensity correction, surface coregistration, spatial smoothing and subcortical segmentation and cortical parcellation based on spherical template registration. Diffusion-weighted images were checked for motion artifact and processed using FreeSurfer's TRACULA and FSL's FDT software (http://www.fmrib.ox.ac.uk/fsl/fdt/index.html).

Tract-of-interest analyses

We defined the tracts of interest using an automated method (FreeSurfer's TRACULA; Yendiki et al., 2012) that defines 18 major white matter tracts in each participant's native diffusion images. This method has been shown to accurately reconstruct tracts in individual subjects by using anatomical priors (based on manual labeling on a separate group of individuals) to guide tractography rather than constrain it; this allows for assessing individual variation while maintaining confidence in choosing the same tract across individuals.

Preprocessing steps included registering DW images to the b = 0 images for motion and eddy current distortions. A two-step registration transform was computed using FreeSurfer's bbregister (Greve, D. et al. 2009) for mapping each participant's b = 0 image to the native structural scan and this to the FSL MNI-152 template. Images were checked for registration errors and no corrections were necessary. White and gray matter masks were generated from each individual's FreeSurfer segmentation and registered to his/her DWI. FSL's DTIFIT was used to estimate tensor fits, which produced Fractional Anisotropy (FA), Axial Diffusivity (AD), and Radial Diffusivity (RD) images (average of the two non-principal eigenvectors). These were then registered to the MNI template space using the registration procedures described above. The manually-labeled training atlas and the individual's white and gray matter masks were then used to estimate priors for each of the major pathways. These also generated end points for the probabilistic tractography as well as control points along the pathway's trajectory. FSL's bedpostX was then used to fit the ball-and-stick model of diffusion to each individual's DWI. Using the anatomical priors

from the training atlas and principal diffusion directions estimated by the ball-and-stick model, probability distributions for each of the major pathways were computed in each individual's native DWIs. After visual inspection, we extracted tract volume, and FA, AD, and RD values averaged over the most probable path per individual.

We examined white matter tracts known to connect critical components of language and reading networks, specifically the inferior longitudinal fasciculus (ILF) and arcuate fasciculus (SLFa), as well as a control tract that is also part of the superior longitudinal fasciculus, but spans the parietal cortex (SLFp). These were examined bilaterally.

Statistical methods

For the TOI analyses, the relationship between diffusion measures and behavioral assessments were tested by means of cross-validation Pearson's correlations, using in-house MATLAB (R2011b; The Mathworks, Natick, MA) code. This cross-validation procedure was implemented in order to assure that the results were not driven by outliers and to increase their applicability to new datasets. Results were considered significant only if they passed $P < 0.05$ for all 20 cross-validation loops. Reported statistical values are the average correlation coefficient r and P across all loops. Control measures included head circumference, age, and each participant's variance in signal-to-noise ratio (SNR) across diffusion gradients, which can be an indicator of movement across these scans.

4.3 Results

We analyzed three tracts bilaterally (**Figure 1**) and performed correlations of volume and diffusivity indices across these tracts with behavioral predictors of dyslexia.

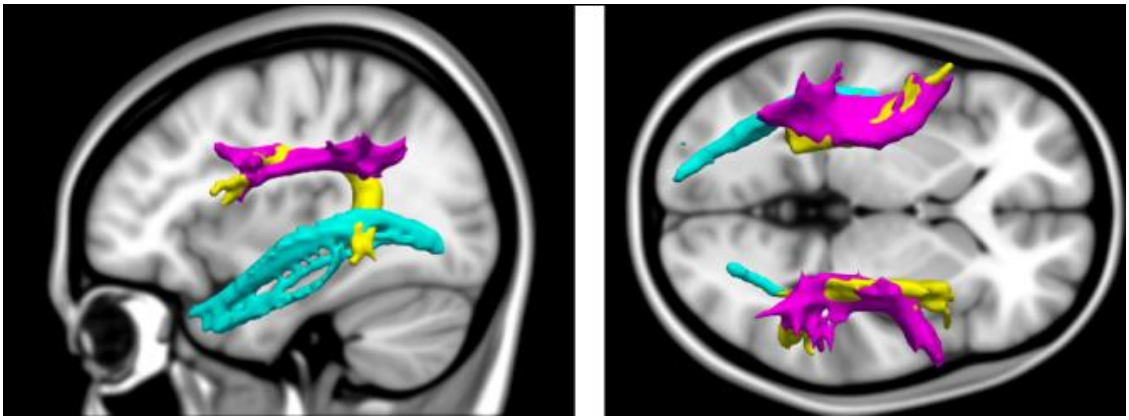

Figure 1. **Illustration of the tracts of interest.** Three bilateral tracts, estimated in each individual's native diffusion space, were extracted from an example participant and registered to MNI template space for visualization here (sagittal view on the left, axial on the right). The inferior temporal fasciculi (cyan) span the occipital and temporal cortices. The arcuate fasciculi (yellow) connect frontal and temporal cortices and are posited to facilitate communication between Broca's and Wernicke's areas. Another component of the superior longitudinal fasciculus, in addition to the arcuate, was also defined as a control tract and illustrated in magenta.

The volume and average axial diffusivity of the left arcuate fasciculus were significantly and positively correlated with individual composite scores on Phonological Awareness (volume: $r = 0.57$, $P = 9.48\text{x}10^{-3}$; axial diffusivity: $r = 0.50$, $P = 2.40\text{x}10^{-2}$). Values from the right arcuate fasciculus and other tracts did not correlate significantly with Phonological Awareness scores. There were no significant correlations with Rapid Automatized Naming or Letter Knowledge ($P > 0.05$). Control measures of head circumference, age, and SNR variance did not correlate with the diffusion measures of the left arcuate fasciculus or any other tract ($P > 0.05$), with the exception that radial diffusivity of the right inferior longitudinal fasciculus, correlated significantly and positively with age ($r = 0.51$, $P = 2.31\text{x}10^{-2}$).

We explored which specific components of the Phonological Awareness composite score (Elision, Blending Words, or Nonword Repetition raw scores) were driving the correlation seen with the left arcuate fasciculus. Scores for Blending Words were correlated with the other measures: $r = 0.62$ with Elision, and $r = 0.60$ with Nonword Repetition (both $P < 0.01$). The volume of the left arcuate fasciculus showed significant positive correlations only with the Blending Words raw scores ($r = 0.61$, $P = 4.08\text{x}10^{-3}$; **Figure 2a**). Blending Words raw scores also correlated with the tract's average fractional anisotropy ($r = 0.55$, $P = 1.29\text{x}10^{-2}$; **Figure 3a**) and average axial diffusivity ($r = 0.60$, $P = 5.30\text{x}10^{-3}$; **Figure 3b**). Three-dimensional renderings of the left arcuate fasciculus tracts, which were ordered by volume and colored by average fractional anisotropy values, illustrated these results (**Figure 2b**). The other components of the Phonological Awareness composite score (Elision and Nonword Repetition) were not significantly correlated with any of the tract's diffusion measures.

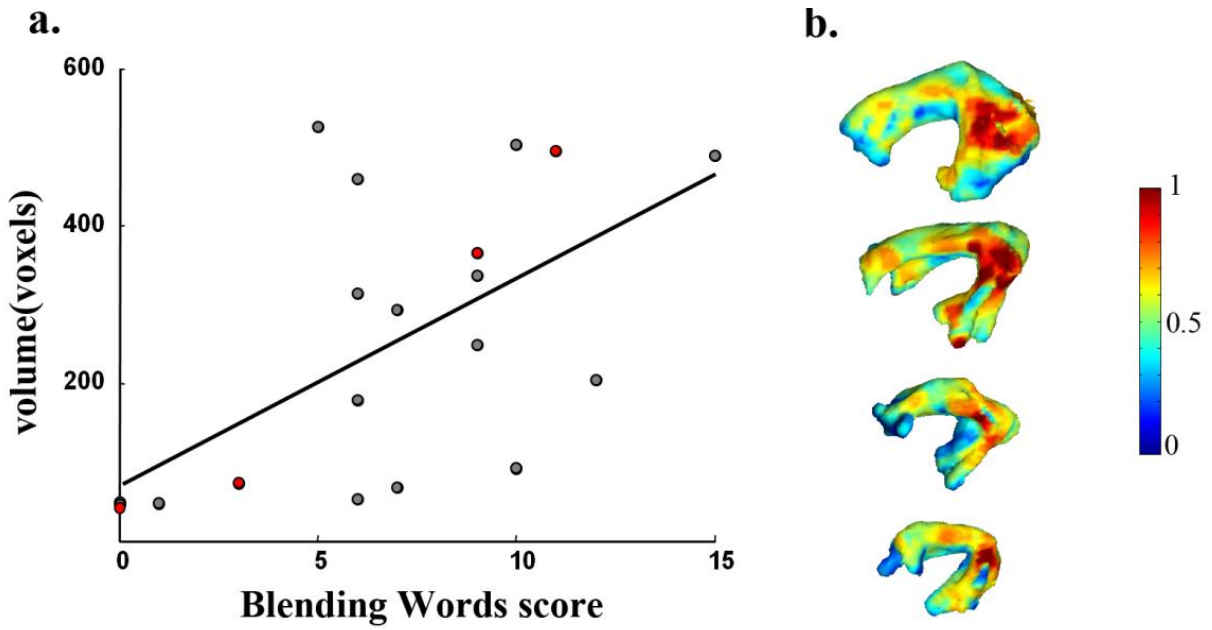

Figure 2. Larger volume of the left arcuate fasciculus is associated with superior Phonological Awareness. a. The volume (number of voxels in diffusion space) of the left arcuate fasciculus is plotted against individual scores of the Blending Words component of the Phonological Awareness composite score. Solid line represents the line of best fit. **b.** To illustrate the relation between the behavioral predictor of dyslexia with left arcuate volume, this tract was rendered from example participants (filled red circles in **a**) and colored according to fractional anisotropy. The tracts are ordered by reading ability (Blending Words score) increasing from bottom to top.

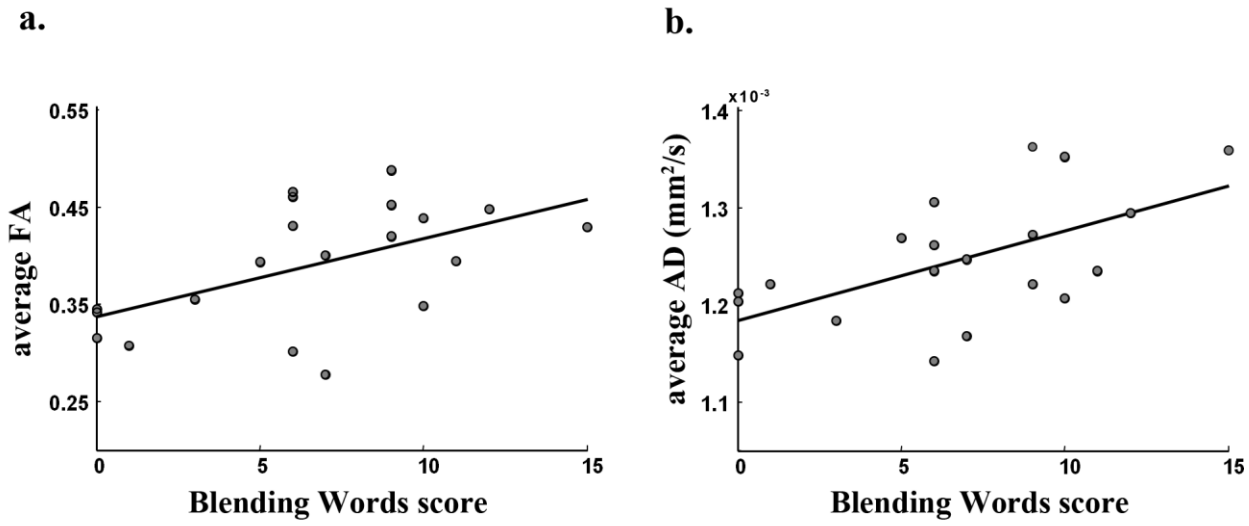

Figure 3. White-matter organization of the left arcuate fasciculus is associated with Blending Words scores. a. Blending Words scores showed a significant positive correlation with the average fractional anisotropy (FA) and **b.** the average axial diffusivity (AD) extracted from each participant's left arcuate fasciculus.

4.4 Discussion

In kindergarten children who had received little or no reading instruction, we found a correlation between Phonological Awareness and several indices of white-matter organization of the left arcuate fasciculus, including volume and axial diffusivity. The correlation was anatomically specific, because it was not observed in five other tracts. The correlation was behaviorally specific, because it was not observed for two other behavioral predictors of dyslexia (Rapid Automatized Naming and Letter Knowledge), and even among phonological measures, it was specific to the Blending Words measure of Phonological Awareness, which measures a child's ability to blend together sounds to form a word. The discovery that such a relation between white-matter organization and one of the strongest behavioral predictors of dyslexia, poor Phonological Awareness, exists prior to reading instruction and substantial reading experience favors the view that differences in white-matter organization are not only the consequence of dyslexia, but also may be a cause of dyslexia.

The association between Phonological Awareness and the left arcuate fasciculus is consistent with the known importance of that tract in connecting left-hemisphere posterior (speech perception) and anterior (speech production) cortical regions important for language, and its correlation with Phonological Awareness in adults (Vandermosten et al., 2012). Reduced indices of white-matter organization could reflect several aspects of white matter tracts. FA is a measure of the amount of anisotropy of water diffusion (e.g. Beaulieu et al., 2009; Mori et al., 2007). Both radial and axial diffusivity are determinants of FA, with axial diffusivity along the principal axis of diffusion more closely associated with axonal

properties such as axon density or number of axons (Beaulieu et al., 2009) than radial diffusivity (average diffusivity for the eigenvectors perpendicular to this principal axis). Measures of diffusivity and anisotropy change with age (Lebel et al. 2008, 2011; Partridge et al., 2004), but this developmental difference was not observable cross-sectionally in the narrow (1-year) age range of our participants, except for radial diffusivity in the right inferior longitudinal fasciculus.

Among the three measures of Phonological Awareness, there was a strong relation between the Blending Words subtest of the CTOPP and both volume and diffusivity measures of the left arcuate fasciculus. This specific correlation likely reflects the relatively challenging nature of this task relative to other tests of Phonological Awareness. In adults, the Blending Words subtest of the CTOPP was more strongly correlated than other CTOPP measures with speeded word reading and word decoding measures (Katz et al., in press). For children, different tests of Phonological Awareness appear to have optimal predictive properties depending on their developmental or psychometric appropriateness. In very young children, simpler tests of Phonological Awareness, such as Rhyme Detection, are the best predictors of later reading ability, but in older children, such as kindergartners, increasingly difficult tasks become better predictors (Adams, 1990; Paris. 2005; Pufpaff, 2009).

There are several limitations to consider in the present study. First, although these children had received no formal reading instruction in school, seven of the children could identify five or more beginning words, and there is evidence that the process of learning to read enhances Phonological Awareness (Cunningham et al. 1998). Correlations were not

calculated for word reading scores because the distribution of the scores was highly skewed; however, single word reading on the WRMT-R Word ID was correlated with the Phonological Awareness measures to a similar degree (Word ID and Blending Words raw scores r = .61). Second, we did not observe DWI correlations with Rapid Automatized Naming or Letter Knowledge. Studies with more participants may have the power to observe such brain-behavior correlations for these predictors of poor reading; alternatively, other structural or functional brain measures will offer more sensitive measures for the other predictors. Third, the correlations we observed are a product of the behaviors we assessed. For example, the inferior longitudinal fasciculus connects regions that may be involved in visual, as opposed to linguistic, aspects of reading and reading-relevant variation may not have been evident in the absence of measures sensitive to visual analysis of print. Fourth, the present study examined DWI differences at a single developmental stage, early kindergarten. As children undergo intensive reading instruction and experience, and vary in their success at reading, white-matter changes may have dynamic developmental properties. For example, weakened left-hemisphere white-matter pathways may reflect a risk and continuing cause for dyslexia, whereas strengthened inter-hemispheric white-matter pathways may reflect adaptive plasticity.

More generally, the present findings support the view that brain differences make learning to read difficult before the commencement of substantial reading instruction and experience. Dyslexia is strongly heritable (Pennington, et al. 1996), and studies have examined brain differences in individuals at familial risk for dyslexia. Newborns at familial risk exhibit differences in event-related potentials (ERPs) to language sounds within hours or days of birth (Guttorm et al., 2001), and longitudinal studies have reported correlations

between such ERP differences during infancy and later language and reading abilities (Molfese et al., 2000; Guttorm et al., 2005). Kindergartners with familial risk for dyslexia have also exhibited structural (Raschle et al., 2011) and functional (Raschle et al., 2012) differences in magnetic resonance imaging studies. Functional brain differences have also been found in kindergartners with better or worse pre-literacy skills (Yamada et al., 2011).

A clinical and educational goal of these sorts of studies is to improve the accuracy by which pre-reading children at risk for dyslexia can be identified so that they can receive early, preventive intervention rather than intervention that follows years of reading failure. Although behavioral measures of Phonological Awareness, Rapid Automatized Naming, and Letter Knowledge in pre-readers predict reading ability years later, the sensitivity and specificity of these behavioral measures is modest. There is some evidence indicating that brain measures substantially enhance the accuracy of predicting reading ability across a school year (Hoeft et al., 2007) or across multiple years (Maurer et al., 2010; Hoeft et al., 2011). The present study indicates that DWI measures of white-matter organization reveal a specific structural risk factor for dyslexia that, in combination with behavioral and other brain measures, may improve the identification of pre-readers at risk for reading difficulty.

4.5 References

Adams, C. (1990). Learning to Read. Cambridge, MA: MIT Press.

Beaulieu, C. (2009). The biological basis of diffusion anisotropy. Diffusion MRI: 105-126.

Dale, A. M., B. Fischl, et al. (1999). Cortical Surface-Based Analysis: I. Segmentation and surface reconstruction. Neuroimage **9**(2): 179-194.

Desikan, R. S., F. Ségonne, et al. (2006). An automated labeling system for subdividing the human cerebral cortex on MRI scans into gyral based regions of interest. Neuroimage **31**(3): 968-980.

Deutsch, G. K., R. F. Dougherty, et al. (2005). Children's reading performance is correlated with white matter structure measured by diffusion tensor imaging. Cortex **41**: 354-363.

Dougherty, R. F., M. Ben-Shachar, et al. (2007). Temporal-callosal pathway diffusivity predicts phonological skills in children. Proceedings of the National Academy of Sciences **104**(20): 8556.

Fischl, B., D. H. Salat, et al. (2002). Whole brain segmentation: automated labeling of neuroanatomical structures in the human brain. Neuron **33**(3): 341-355.

Fischl, B., A. van der Kouwe, et al. (2004). Automatically parcellating the human cerebral cortex. Cereb Cortex **14**(1): 11-22.

Frye, R. E., J. Liederman, et al. (2011). Diffusion tensor quantification of the relations between microstructural and macrostructural indices of white matter and reading. Human brain mapping **32**(8): 1220-1235.

Gabrieli, J. D. E. (2009). Dyslexia: a new synergy between education and cognitive neuroscience. Science **325**(5938): 280-283.

Guttorm, T. K., P. H. T. Leppänen, et al. (2005). Brain event-related potentials (ERPs) measured at birth predict later language development in children with and without familial risk for dyslexia. Cortex **41**(3): 291-303.

Guttorm, T. K., P. H. T. Leppänen, et al. (2001). Event-related potentials and consonant differentiation in newborns with familial risk for dyslexia. Journal of Learning Disabilities **34**(6): 534-544.

Greve, D., Fischl, B. (2009). Accurate and robust brain image alignment using boundary-based registration. Neuroimage **48**: 63-72.

Hoeft, F., B. D. McCandliss, et al. (2011). Neural systems predicting long-term outcome in dyslexia. Proceedings of the National Academy of Sciences **108**(1): 361-366.

Hoeft, F., A. Meyler, et al. (2007). Functional and morphometric brain dissociation between dyslexia and reading ability. Proceedings of the National Academy of Sciences **104**(10): 4234.

Katz, L., L. Brancazio, et al. (in press). What lexical decision and naming tell us about reading. Reading and Writing.

Klingberg, T., M. Hedehus, et al. (2000). Microstructure of temporo-parietal white matter as a basis for reading ability: Evidence from diffusion tensor magnetic resonance imaging. Neuron **25**(2): 493-500.

van der Kouwe, A.J., Benner, et al. (2008). Brain morphometry with multiecho MPRAGE. Neuroimage **40**: 559-569.

Lebel, C. and C. Beaulieu (2011). Longitudinal development of human brain wiring continues from childhood into adulthood. The Journal of Neuroscience **31**(30): 10937-10947.

Lebel, C., L. Walker, et al. (2008). Microstructural maturation of the human brain from childhood to adulthood. Neuroimage **40**(3): 1044-1055.

Lyon, G. R., S. E. Shaywitz, et al. (2003). A definition of dyslexia. Annals of dyslexia **53**(1): 1-14.

Maurer, U., E. Schulz, et al. (2010). The development of print tuning in children with dyslexia: Evidence from longitudinal ERP data supported by fMRI. Neuroimage.

Molfese, D. L. (2000). Predicting dyslexia at 8 years of age using neonatal brain responses. Brain and Language **72**(3): 238-245.

Mori, T., T. Ohnishi, et al. (2007). Progressive changes of white matter integrity in schizophrenia revealed by diffusion tensor imaging. Psychiatry Research: Neuroimaging **154**(2): 133-145.

Mugler, J.P., 3rd, Bao, S., et al. (2000). Optimized single-slab three-dimensional spin-echo MR imaging of the brain. Radiology **216**: 891-899.

Paris, S. G. (2005). Reinterpreting the development of reading skills. Reading Research Quarterly **40**(2): 184-202.

Partridge, S. C., P. Mukherjee, et al. (2004). Diffusion tensor imaging: serial quantitation of white matter tract maturity in premature newborns. Neuroimage **22**(3): 1302-1314.

Pennington, B. F. & Gilger, J. W. (1996). How is dyslexia transmitted? Neural, cognitive, and genetic mechanisms. In: C.H. Chase, G. D. Rosen and G. F. Sherman (Eds.), Developmental Dyslexia, York Press, MD, pp. 41-61.

Pufpaff, L. A. (2009). A developmental continuum of phonological sensitivity skills. Psychology in the Schools **46**(7): 679-691.

Raschle, N. M., M. Chang, et al. (2011). Structural brain alterations associated with dyslexia predate reading onset. Neuroimage **57**(3): 742-749.

Raschle, N. M., J. Zuk, et al. (2012). Functional characteristics of developmental dyslexia in left-hemispheric posterior brain regions predate reading onset. Proceedings of the National Academy of Sciences **109**(6): 2156-2161.

Rimrodt, S. L., D. J. Peterson, et al. (2010). White matter microstructural differences linked to left perisylvian language network in children with dyslexia. Cortex **46**(6): 739-749.

Schatschneider, C., J. M. Fletcher, et al. (2004). Kindergarten prediction of reading skills: A longitudinal comparative analysis. Journal of Educational Psychology **96**(2): 265.

Shaywitz, B. A., S. E. Shaywitz, et al. (2002). Disruption of posterior brain systems for reading in children with developmental dyslexia. Biological psychiatry **52**(2): 101-110.

Shaywitz, S. E. and B. A. Shaywitz (2005). Dyslexia (specific reading disability). Biological Psychiatry **57**(11): 1301-1309.

Snowling, M., S. Stothard, et al. (2009). The York Assessment of Reading for Comprehension.

Stanovich, K. and A. Cunningham (1998). What reading does for the mind. American Educator **22**: 8-15.

Steinbrink, C., K. Vogt, et al. (2008). The contribution of white and gray matter differences to developmental dyslexia: insights from DTI and VBM at 3.0 T. Neuropsychologia **46**(13): 3170-3178.

Tanaka, H., J. M. Black, et al. (2011). The Brain Basis of the Phonological Deficit in Dyslexia Is Independent of IQ. Psychological science **22**(11): 1442-1451.

Tisdall, M. D., A. T. Hess, et al. (2011). Volumetric navigators for prospective motion correction and selective reacquisition in neuroanatomical MRI. Magnetic Resonance in Medicine.

Vandermosten, M., B. Boets, et al. (2012). A tractography study in dyslexia: neuroanatomic correlates of orthographic, phonological and speech processing. Brain **135**(3): 935-948.

Wagner, R. K., J. K. Torgesen, et al. (1999). Comprehensive Test of Phonological Processing, Austin, TX: Pro-Ed.

Wolf, M. and M. B. Denckla (2005). RAN/RAS: Rapid automatized naming and rapid alternating stimulus tests. Austin, TX: Pro-Ed.

Woodcock, R. W. (1987). Woodcock Reading Mastery Tests-Revised/Normative Update, American Guidance Service Circle Pines, MN.

Yamada, Y., C. Stevens, et al. (2011). Emergence of the neural network for reading in five-year-old beginning readers of different levels of pre-literacy abilities: An fMRI study. Neuroimage **57**(3): 704-713.

Yendiki, A., P. Panneck, et al. (2011). Automated probabilistic reconstruction of white-matter pathways in health and disease using an atlas of the underlying anatomy. Frontiers in Neuroinformatics **5**(23).

Chapter 5

Conclusions

A fundamental and yet unanswered question in neuroscience is "what are the neuroanatomical constraints on the development of function and behavior?" Neuroimaging research now has the appropriate tools to integrate anatomical connectivity with functional mapping (e.g. Saygin, Osher et al. 2012), and can therefore make major steps to understand the biological underpinnings of human function and behavior. By trying to answer this fundamental question, we can advance the specificity with which neuroimaging can propose mechanistic and explanatory principles, experimentally test these principles, and make predictions of its outcome based on perturbance or differing experience. In this thesis, I started by referring to work in non-human primates (which have the advantage of invasive experimental manipulation) to identify structural markers in the human brain, then tested the maturation of these markers, and proposed some mechanisms by which structural changes may shape future function.

5.1 Connectivity fingerprints of fine-grained anatomy

We know from non-human animal studies that amygdala nuclei each have characteristic connectivity patterns, which subserve unique functions. In humans, these nuclei are unfortunately difficult to visualize using standard, non-invasive anatomical imaging methods; therefore, much is unknown about their functions, as well as their connectivity patterns. In Chapter 2, I proposed a new method of using known structural connectivity patterns, based on rat and non-human primate studies, to define subject-specific amygdaloid subregions in humans. I showed that these regions correspond to the known locations of the nuclei based on histology, as well as to a high-resolution MR scan on which nucleic boundaries are visible. The subregions were also spatially consistent across thirty-five individuals.

A current extension of this project involves high-resolution imaging of post-mortem brain samples on a 7-Tesla scanner, giving us great resolution to visualize even finer boundaries in the amygdala (Saygin, Kliemann et al., in progress). These post-mortem specimens are scanned over many hours, usually an entire weekend, resulting in much higher spatial resolution and better image signal than is possible for in-vivo scans. The resulting 100μm images are then manually labeled into ten amygdala nuclei, and validated through histology. We then hope to use DWI and tractography to explore the connectivity patterns of the nuclei and compare these to the patterns of connectivity that were used in the current project, which were based off of animal studies.

TractSeg can also be applied to any gray matter structure, even though I demonstrated a specific application to the amygdala in this thesis. For example, the nuclei of the basal ganglia also have very characteristic connectional patterns, which could easily be conglomerated with Boolean expressions. A recent study used functional connectivity, or correlations of non-task related BOLD responses between brain regions, to segment the basal ganglia into its nuclei (Di Martino, Scheres, et al. 2008; Lenglet, Abosch, et al. 2012). It will be interesting to compare these results to those obtained using structural connectivity with DWI (see Zhang, Snyder et al. 2010 for an example of this comparison for the thalamic nuclei). Establishing connectivity fingerprints will then allow researchers to constrain the search-space of pathways to only those that delineate cytoarchitectonic boundaries. For example, if a pair of anatomically disparate regions differ functionally, and also possess distinct connectivity fingerprints, then it may be the distinctions within those fingerprints that underlie the functional differences. The functionally relevant aspects of these connectivity fingerprints can then be realized, bringing us closer to functional connectomics, as explained in the next section.

5.2 Functional implications of connectivity fingerprints

The connectivity fingerprints of amygdala nuclei (as defined by TractSeg) can be used to create regions of interest, or ROIs. These ROIs can then be used to explore the functional roles of the distinct nuclei within the human amygdala. So far, nucleic function has only been approximated using template-based atlases which require warping of

neuroanatomy or visual approximation (e.g. Morris, Buchel, et al. 2001; Etkin, Klemenhagen, et al. 2004). These methods can lead to loss of information from warping (or worse, incorrect conclusions if the region ends up mapping to a completely different place), or can be incredibly labor-intensive. TractSeg is a better alternative because it relies on subject-specific connectivity patterns using rapid diffusion sequences that can be easily introduced into experimental paradigms. Further, it can be used to study any functional anomalies in these nuclei in clinical populations for which the amygdala as a whole has been implicated (Phillips, Drevets, et al. 2003).

But, perhaps even more importantly, these fingerprints can be 'weighted' in terms of their importance in defining the specific function of each nucleus. Although the function of any brain region is largely determined by its connectivity patterns, not all the connections are relevant in every function. Each connection has a different relative weight in producing a given function of that region, which describes the region's functional connectome. I have explored this concept in relation to face selectivity in the fusiform gyrus: by using only structural connectivity, as measured through DWI, we were able to predict functional activation to faces in the fusiform gyrus in two separate groups of participants (Saygin, Osher et al. 2012). This study identifies cortical regions whose connectivity is highly influential in predicting face-selectivity within the fusiform, suggesting a possible mechanistic architecture underlying face processing in humans. A similar analysis could be performed on the functional responses of the amygdala nuclei in order to compare not only the structural connectivity fingerprints but also their relative importance in predicting functional responses. These types of studies will elucidate the functional relevance of

anatomical connections and thus better inform us of the mechanisms of functional activation, and eventually, of human behavior.

5.3 Ontogeny of connectivity fingerprints: possible biological mechanisms and functional implications

Given its important role in *early* social learning in non-human primates (e.g. Thompson, Schwartzbaum, et al. 1969; Prather, Lavenex, et al. 2001), and functional activation differences in the human amygdala of children vs. adults (e.g. Killgore and Yurgelun-Todd 2006; Monk, McClure, et al. 2003; Thomas, Drevets, et al. 2001), it is possible that the connectivity fingerprints discovered by TractSeg only apply to the mature amygdala; perhaps the amygdala nuclei's connectivity patterns change with normal development and experience. In chapter 3, I explored the developmental trajectory of the amygdala as a whole and of its four nuclei. I found that the whole amygdala is connected with more brain regions in children than in adults, and that this developmental difference was specific to the basal and lateral nuclei of the amygdala.

These results suggest that the pruning of specific connectivity patterns is perhaps one of the mechanisms by which functional maturation occurs in the amygdala. Several possible mechanisms could be at play in order to achieve the final state of the adult brain, and each could have separate functional implications. These mechanisms include cell death, growth of dendritic spines, and the remodeling of connections, which can be in the

form of refinement or elimination, and are both attributable to the pruning of branched axonal collaterals maintained into adulthood. Both forms of remodeling have been previously shown to occur in the amygdala's connections with the temporal cortex (Webster, Ungerleider et al. 1991a,b). Refinement occurs when projections become more restricted through development; they initially terminate in the functionally appropriate brain region, but are more widespread in childhood. Elimination is the retraction of projections during development and occurs when projections terminate in a functionally anomalous region.

The amygdala findings outlined in the present thesis confirm that these two processes of connectivity remodeling occur in the basal and lateral nuclei of the *human* amygdala, and extend it to show that these processes occur for both amygdala-cortical and amygdala-subcortical connectivity. Further, I reported that an increase in connectivity also exists between these nuclei and the rest of the medial temporal cortex, possibly through the growth of new dendritic spines or increased axonal packing and alignment.

Specifically, the connectivity of the basal and lateral nuclei with certain subcortical brain regions, like the basal ganglia, was found to decrease with age, while connectivity with the hippocampus increased. The basal and lateral nuclei resemble the hippocampus cytoarchitectonically, whereas the other nuclei resemble striatal cytoarchitecture. The decreasing connectivity between the basal/lateral nuclei and basal ganglia may reflect their separation from striatal circuitry; the mechanism by which this occurs would then be elimination rather than refinement. Conversely, their increasing integration with the hippocampus may reflect their increasing assimilation with medial temporal circuitry, and

may be functionally relevant in forming the adult network that subserves emotional memory. A recent study in rats found that the basolateral amygdala is necessary for the integration of new cells into emotional memory networks (Kirby, Friedman et al. 2012), and thus provides evidence for the hypothesis that the increase in connectivity with the hippocampus may be the mechanism by which this function develops in humans as well.

I also presented evidence in favor of pruning via refinement rather than elimination. The experiments in Chapter 3 showed that the basal and lateral nuclei decreased in their connectivity patterns with cortical regions involved in emotional and social processing (e.g. TPJ). This decrease in connectivity may reflect the basolateral amygdala's early role in learning and relaying appropriate social information to other cortices; perhaps these nuclei have an early instructional role in their connectivity patterns, and this role changes as the connectivity patterns become increasingly specific, with increasing functional specialization in regions with which it's connected, such as the TPJ.

Existing structural variation is shaped by experience through postnatal pruning, which influences specialization of function. Structural remodeling could generate not only regional diversity, but also individual variation (O'Leary 1992; Luo and O'Leary 2005; Tamnes, Fjell, et al. 2012). Indeed, amygdala connectivity in our study was quite variable in children as compared to adults, especially in the basal and lateral nuclei. Non-human primate literature on amygdala evolution suggests that the size of these two nuclei, and their sociovisual cortical targets, correlate positively with social group size (Barton and Aggleton 2000). As mentioned above, amygdala connections with sociovisual temporal cortices undergo specialization through development, and these changes occur in tandem

with increases in social behavior (Kalin, Shelton, et al. 1991). Although the nuclei did not differ in size across development (Chapter 3), inter-subject variability of basal/lateral connectivity became more consistent with development. Perhaps the functional specialization of the social brain is more variable across children than adults, due to the vast differences across individuals in the quantity/quality of social experience in childhood and the interaction of this experience with pre-wired structural constraints. Such hypotheses on the functional implication of the structural remodeling of the nuclei, remain to be tested.

5.4 Testable hypotheses of the ontogeny of amygdala structure and function

As suggested in Chapter 1, studies that integrate structural and developmental approaches can provide hypotheses for biological mechanisms of function and behavior. I have provided such hypotheses for possible functional implications of the amygdala's structural maturation. These hypotheses can be tested by integrating anatomical connectivity measures with fMRI in the same individuals and studied across development. For example, future studies could focus on regions whose amygdalar connectivity changes with age; it would be interesting to assess the spatial distribution of amygdalar connectivity within these regions, directly relate this to the spatial distribution of function (e.g. Saygin, Osher et al. 2012), and test how this changes with age. One would hypothesize, based on the results of Chapter 3, that the spatial map of connectivity to the

amygdala from these cortices would be increasingly focalized, and overlap well with functionally specific regions such as the fusiform face area (Kanwisher, McDermott et al. 1997; Tsao, Freiwald et al. 2006) or the TPJ (Saxe and Kanwisher 2003). This will provide insight into the functional consequences of these connectivity changes in normal development, and help formalize more informed hypotheses about which regions or connections are specifically impaired by limited or pathological social interactions during human development.

Another possible extension would be to establish connectional fingerprints that account for age, for each of the amygdaloid nuclei. Given the different maturation rates for each nucleus' connectivity with other brain regions, a regression analysis could be used to model the relative contribution of these connectivity patterns to age. The resulting model coefficients could be used to transform the connectivity data in order to normalize them with respect to age. Alternatively, these coefficients could be incorporated into fuzzy logical expressions, which allow for continuous, rather than discrete, values of "truth." The connectivity-based amygdala segmentations should then be valid for all ages studied. By constructing such age-specific segmentation expressions of connectivity, one can then propose a connectivity fingerprint of maturation for the amygdala, which can later be explored in relation to functional maturation of the region or other regions with which it is connected.

5.5 Structural connectivity constraints on future behavior

I reported in Chapter 4 that greater white matter integrity of the left arcuate fasciculus, as measured by volume and axial diffusivity, is related to superior phonological awareness, which in turn is a strong predictor of reading ability and risk of dyslexia. Among the three measures of phonological awareness, the Blending Words subtest was especially related to volume, axial diffusivity, and fractional anisotropy of the left arcuate fasciculus. These measures of white matter integrity may reflect axonal packing and density rather than myelination (which is better measured through radial diffusivity; see Beaulieu 2009). How are larger volume and greater axonal packing related to better reading ability, in light of the pruning-based changes that were described for the amygdala nuclei? Both processes probably co-occur in support of specialized function by generating better organization of fibers. The mechanisms of elimination, refinement, and growth may all reflect fiber optimization, and I propose that they reflect the structural basis underlying the observed individual variation in phonological awareness.

The proposed structural basis of later reading ability (integrity of the left arcuate) can be tested longitudinally. The influence of experience and plasticity might be measurable in children that had low tract integrity but do not develop dyslexia, which could be manifest either as an increase in the volume/AD of their arcuate (catch-up growth) or as a compensatory change elsewhere. Further, if the pre-reading measures of tract integrity remain highly correlated with later reading ability, an intervention study

involving phonological awareness training could be conducted to perturb the system and probe the mechanisms by which structure constrains functional development. Do children trained on phonological awareness catch up more than children trained on other behavioral metrics, in terms of reading ability *and* arcuate integrity? This is a testable outcome which could extend and solidify the dynamic relationship between structure and function across development as proposed in this thesis. Furthermore, pre-reading predictors, including anatomical ones, could be used to better refine specialized education, perhaps even before children begin learning to read, which in the best case scenario may prevent dyslexia.

5.6 Conclusion

Although their theories have risen or fallen, the most influential figures throughout the history of neuroscience have inspired progress by proposing biological mechanisms for cognition, using whatever tools they had at the time. Advances in neuroimaging now give us the ability to link anatomical observations with cognitive assessments in the developing human; neuroscientists presently possess an unprecedented ability to surmount mere mapping and description of brain function and can now propose and test the mechanics of the mind. This thesis has proposed some ways in which the conjunction of structure, function, and developmental approaches can bring us closer to an understanding of the mature nervous system and how it produces human cognition.

5.7 References

Amaral, D. G. (1986). "Amygdalohippocampal and amygdalocortical projections in the primate brain." Adv Exp Med Biol **203**: 3-17.

Beaulieu, C. (2009). "The biological basis of diffusion anisotropy." Diffusion MRI: 105-126.

Di Martino, A., Scheres, A., Margulies, D. S., Kelly, A. M., Uddin, L. Q., Shehzad, Z., Biswal, B., Walters,J R., Castellanos, F. X. & Milham, M. P. (2008). "Functional connectivity of human striatum: a resting state FMRI study." Cereb Cortex, 18**,** 2735-47.

Etkin, A., Klemenhagen, K., Dudman, J. T., Rogan, M. T., Hen, R., Kandel, E., Hirsch, J. (2004). "Individual differences in trait anxiety predict the response of the basolateral amygdala to unconsciously processed fearful faces". Neuron, **44**: 1043-55.

Kalin, N., Shelton, S., and Takahashi, L. (1991). "Defensive behaviors in infant rhesus monkeys: ontogeny and context dependent selective expression." Child Development **62**(5): 1175-1183.

Killgore, W. & Yurgelun-Todd, D. (2006). "Ventromedial prefrontal activity correlates with depressed mood in adolescent children." Neuroreport **17**, 167-171.

Kirby, E., A. Friedman, Covarrubias, D, Ying C, Sun, WG, Goosens, KA, Sapolsky, RM, Kaufer D. (2012). "Basolateral amygdala regulation of adult hippocampal neurogenesis and fear-related activation of newborn neurons." Molecular Psychiatry. **17**(5):527-36.

Lenglet, C., Abosch, A., Yacoub, E., De Martino, F., Sapiro, G., and Harel, N. (2012). "Comprehensive in vivo Mapping of the Human Basal Ganglia and Thalamic Connectome in Individuals Using 7T MRI." PloS one **7**(1): e29153.

Luo, L. and D. D. M. O'Leary (2005). "Axon retraction and degeneration in development and disease." Annu. Rev. Neurosci. **28**: 127-156.

Monk, C.S., McClure, E.B., Nelson, E.E., Zarahn, E., Bilder, R.M., Leibenluft, E., Charney, D.S., Ernst, M., Pine, D.S. (2003). "Adolescent immaturity in attention-related brain engagement to emotional facial expressions." Neuroimage **20**, 420-428.

Morris, J. S., Buchel, C., and Dolan, R.J. (2001). "Parallel neural responses in amygdala subregions and sensory cortex during implicit fear conditioning." Neuroimage **13**(6): 1044-1052.

O'Leary, D. D. M. (1992). "Development of connectional diversity and specificity in the mammalian brain by the pruning of collateral projections." Current Opinion in Neurobiology **2**(1): 70-77.

Phillips, M. L., Drevets, W. C., Rauch, S. L., and Lane, R. (2003). "Neurobiology of emotion perception II: Implications for major psychiatric disorders". Biol Psychiatry, **54**: 515-28.

Prather, M., Lavenex, P., Mauldin-Jourdain, M.L., Maso,n W.A., Capitanio, J.P., Mendoza, S.P., and Amaral, D.G. (2001). "Increased social fear and decreased fear of objects in monkeys with neonatal amygdala lesions." Neuroscience **106** (4): 653-658.

Saygin, Z. M., Osher, D. E., Koldewyn, K., Reynolds, G., Gabrieli, J. D. E., & Saxe, R. R. (2012). "Anatomical connectivity patterns predict face selectivity in the fusiform gyrus." Nature Neuroscience (**15**), 321-327.

Saygin Z. M., Kliemann D., Huber, K., Reuter, M., Player, A.S., Gabrieli J.D.E., *Fischl B., *Augustinack J. (in progress). "Human amygdala subnuclei as revealed through high-resolution MRI."

Tamnes, C. K., Fjell, A. M., Westlye, L.T., Østby, Y., Walhovd, K.B. (2012). "Becoming Consistent: Developmental Reductions in Intraindividual Variability in Reaction Time Are Related to White Matter Integrity." Journal of Neuroscience **32**(3): 972-82.

Thomas, K., Drevets, W.C., Whalen, P.J., Eccard, C.H., Dahl, R.E., Ryan, N.D., Casey, B.J. (2001). Amygdala response to facial expressions in children and adults. Biological Psychiatry **49**, 309-316.

Thompson, C.I., Schwartzbaum, J. S., Harlow, H. F. (1969). "Development of social fear after amygdalectomy in infant rhesus monkeys." Physiology & Behavior **4** (2): 249-254.

Webster, M., Ungerleider, L., Bachevalier J. (1991a). "Connections of inferior temporal areas TE and TEO with medial temporal-lobe structures in infant and adult monkeys." Journal of Neuroscience **11**(4): 1095-1116.

Webster, M. J., Ungerleider, L., Bachevalier J. (1991b). "Lesions of inferior temporal area TE in infant monkeys alter cortico-amygdalar projections." Neuroreport: An International Journal for the Rapid Communication of Research in Neuroscience.

Zhang, D., Snyder, A. Z., Shimony, J.S., Fox, M.D., Raichle, M.E. (2010). "Noninvasive functional and structural connectivity mapping of the human thalamocortical system." Cerebral Cortex **20** (5): 1187-1194.